RUSSIAN ACADEMY OF SCIENCES
Физический институт имени П.Н.Лебедева
Ф И А Н

ISTC Project No. 3835-P

Study of factors determining the gain characteristics of DOIL active medium

Final Project Technical Report

on the work performed from March 01, 2008 to February 28, 2009

P.N.Lebedev Physical Institute of Russian Academy of Sciences,
N.G.Basov Quantum Radiophysics Institute

Project Manager **Ionin Andrey Alekseevich, Professor**

Director **Krokhin Oleg Nikolaevich Academician**

March 2009

This work was supported financially by EOADR and performed under the agreement with the International Science and Technology Center (ISTC), Moscow.

March 2009

This work was supported financially by EOADR and performed under the agreement with the International Science and Technology Center (ISTC), Moscow.

REPORT DOCUMENTATION PAGE

Form Approved OMB No. 0704-0188

1. REPORT DATE *(DD-MM-YYYY)*	2. REPORT TYPE	3. DATES COVERED *(From – To)*
17-04-2009	Final Report	01-Mar-08 - 17-Apr-09

4. TITLE AND SUBTITLE

Study of Factors Determining the Gain Characteristics of DOIL Active Medium

5a. CONTRACT NUMBER
ISTC Registration No: 3835

5b. GRANT NUMBER

5c. PROGRAM ELEMENT NUMBER

6. AUTHOR(S)

Professor Andrey Alekseevich Ionin

5d. PROJECT NUMBER

5d. TASK NUMBER

5e. WORK UNIT NUMBER

7. PERFORMING ORGANIZATION NAME(S) AND ADDRESS(ES)

Lebedev Physics Institute
53 Leninsky Prospect
Moscow 119991
Russia

8. PERFORMING ORGANIZATION REPORT NUMBER

N/A

9. SPONSORING/MONITORING AGENCY NAME(S) AND ADDRESS(ES)

EOARD
Unit 4515 BOX 14
APO AE 09421

10. SPONSOR/MONITOR'S ACRONYM(S)

11. SPONSOR/MONITOR'S REPORT NUMBER(S)
ISTC 06-7006

12. DISTRIBUTION/AVAILABILITY STATEMENT

Approved for public release; distribution is unlimited.

13. SUPPLEMENTARY NOTES

14. ABSTRACT

The aim of the Project is to study experimentally and theoretically the possibility of working pressure increase and increase of singlet delta oxygen (SDO) yield in conditions of gas flow through the discharge region. Also, the properties of SDO and iodine containing gas mixture will be studied during the Project. In this connection, creation of experimental discharge facilities with gas flow is needed for efficient SDO production. During the work on the Project, active gas mixture will be formed by mixing of SDO obtained in the discharge and iodine donor with following iodine donor photo dissociation. Experiments on this active gas mixture parameters optimization will be carried out by studying its characteristics in pulsed mode. Also, available theoretical model should be developed to cover reactions with iodides and gas dynamic effects in SDO and iodine containing gas mixture flow.

These experiments, carried out both in static conditions and with gas flow, are very important for modeling conditions of real electric discharge SDO production systems. Secondly, a study of a technique of compulsory atomic iodine production will be accomplished. Some products, which are produced in oxygen containing discharge plasma, could make it more difficult to form mixture of iodine donor and SDO obtained in the discharge. Minimization of such negative influence will allow high concentration of iodine atoms at low pressure of the gas mixture. Thirdly, theoretical modeling of the processes in gas flow containing SDO and iodine mixture will be carried out. Development of the theoretical model by including reactions with iodides and gas dynamic effects is of great interest for complete description of electric discharge SDO production systems and numerical optimization of its parameters.

15. SUBJECT TERMS

EOARD, Physics, Plasma Physics and Magnetohydrodynamics

16. SECURITY CLASSIFICATION OF:			17. LIMITATION OF ABSTRACT	18, NUMBER OF PAGES	19a. NAME OF RESPONSIBLE PERSON
a. REPORT	b. ABSTRACT	c. THIS PAGE			A. GAVRIELIDES
UNCLAS	UNCLAS	UNCLAS	UL	53	19b. TELEPHONE NUMBER *(Include area code)* +44 (0)1895 616205

Title of the Project:	Study of factors determining the gain characteristics of DOIL active medium
Commencement Date:	March 01, 2008
Duration:	12 months
Project Manager	Ionin Andrey Alekseevich
phone number:	+7 (499) 783-36-90
fax number:	+7 (499) 783-36-90
e-mail address:	aion@sci.lebedev.ru
Leading Institute:	P.N.Lebedev Physical Institute of Russian Academy of Sciences, N.G.Basov Quantum Radiophysics Institute Leninskii pr., 53, Moscow, 119991 Russia Phone: +7 (495) 135-14-29 E-mail: postmaster@sci.lebedev.ru URL: http://www.lebedev.ru

Keywords: singlet delta oxygen, RF discharge, e-beam sustained discharge, slab discharge, gas flow**,** nitrogen oxide, relaxation constant, temperature dependence, iodine atom, pulse-periodic mode, kinetic model.

LIST OF PARTICIPANTS

1. **Ionin Andrey Alekseevich,** Professor, Project Manager
2. **Napartovich Anatoliy Petrovich,** Professor
3. **Yuryshev Nikolay Nikolaevich,** Dr**.**
4. **Kochetov Igor' Valerianovich,** Dr**.**
5. **Kotkov Andrey Aleksandrovich,** Dr**.**
6. **Klimachev Yuriy Mikhaylovich,** Dr**.**
7. **Sinitsyn Dmitriy Vasil'evich,** Dr**.**
8. **Seleznev Leonid Vladimirovich,** Dr**.**
9. **Vagin Nikolay Pavlovich,** Dr**.**
10. **Ionina Nina Anatol'evna**
11. **Kozlov Andrey Yur'evich**
12. **Rulev Oleg Alekseevich**

LIST OF CONTENTS

1. Brief description of the work plan: objective, expected results, technical approach 5
1.1 Introduction and Overview 5
1.2 Scope of Activities 6
1.3 Technical Approach and Expected Results 7
2. Methods, Experiments, Theory, Results. 8
2.1. SDO production in pulsed EBSD and slab RF discharge 8
2.1.1. SDO production in pulsed EBSD and slab RF discharge without gas flow 8
2.1.2. SDO production in slab RF discharge with gas flow 13
2.2. Possibility study of a technique of compulsory atomic iodine production. 32
3. Conclusions. 46
4. References. 47
Attachment 1: List of published papers and reports with abstracts. 49
Attachment 2: List of presentations at conferences and meetings with abstracts. 51
Attachment 3: Information on patents and copyrights. 53

1. Brief description of the work plan: objective, expected results, technical approach

1.1. Introduction and Overview

In our previous research carried out under the ISTC partner Project #2415-P, electric discharge and its afterglow kinetics were studied experimentally and theoretically for gas mixtures containing oxygen (*Ionin A.A., 2006a*). The main results of the study were obtained using experimental facilities operating at static conditions i.e. without gas flow. This circumstance restricts the applicability of the results obtained for the development of real discharge systems for efficient singlet delta oxygen (SDO) production and its parameters optimization. It is known (*Rakhimova T.V., 2003*) that significant amount of atomic oxygen (which is a strong SDO quencher) is produced in electric discharge ignited in oxygen containing gas mixtures. Also it was shown in (*Fujii H., 2003*) that small addition of NO leaded to atomic oxygen concentration decrease. This fact may be used for decreasing SDO losses during its transportation. Gas mixture properties are defined, besides SDO content, by created concentration of iodine atoms. The method of pulsed volumetric iodine atoms generation (*Yuryshev N.N., 2001*) was presented itself in a good light and being used may create high concentration of iodine atoms just at low gas pressure and at not very high SDO content. Theoretical study under the ISTC partner Project #2415-P was devoted to creation of full kinetic model describing processes responsible for SDO production in different electric discharges. Such a model was completed and tested by comparison of calculated data and experimental results (*Ionin A.A., 2006b*).

The aim of the new Project was to study experimentally and theoretically the possibility of working pressure increase and SDO yield raising in conditions of gas flow through the discharge region. Also, the properties of SDO and iodine containing gas mixture were studied during the Project. In this connection, creation of experimental discharge facilities with gas flow was needed for efficient SDO production. During the work on the Project, active gas mixture was formed by mixing of SDO obtained in the discharge and iodine donor with following iodine donor photo dissociation. Experiments on this active gas mixture parameters optimization were carried out by studying its characteristics in pulsed mode. Also, available theoretical model was developed to cover reactions with iodides and gas dynamic effects in SDO and iodine containing gas mixture flow.

The work on the Project was divided into three Tasks that were solved in parallel.

- The study of SDO production in slab RF discharge.
  These experiments, being carried out both in static conditions and with gas flow, are very important for modeling conditions of real electric discharge SDO production systems.
- Possibility study of a technique of compulsory atomic iodine production.
  Some products, which are produced in oxygen containing discharge plasma, could make more difficult to form mixture of iodine donor and SDO obtained in the discharge. Minimization of such negative influence obtains high concentration of iodine atoms just at low pressure of the gas mixture.
- Theoretical modeling of the processes in gas flow containing SDO and iodine mixture.
  Development of the theoretical model by including reactions with iodides and gas dynamic effects is of great interest for complete description of electric discharge SDO production systems and numerical optimization of its parameters.

The research team proposed for this Project consists of experts from the Gas Laser Lab and Chemical Lasers Lab of the Lebedev Physics Institute. The research team has extensive experience in the field of experimental and theoretical fundamental research on kinetic

processes taking place in low temperature plasma produced in different electric discharges, and in chemical reactions.

1.2. Scope of Activities

The activity on the Project was directed on three main Tasks that were being solved in parallel. Each task was subdivided into four subtasks that were solved consequently within the period of three months (one quarter).

Task A. The study of SDO production in slab RF discharge.

For the first time electrically generated SDO yield above threshold value was obtained with exciting of oxygen containing gas mixture by RF discharge and following cooling of the mixture in supersonic gas flow. With gas mixture exciting by electric discharge the gas temperature increases. Therefore the active gas mixture temperature decreasing is necessary. From this point of view, slab discharge geometry is very attractive since effective diffusion and convective gas cooling is available. Moreover, in slab geometry gas cooling down to cryogenic temperature is possible without supersonic gas flow. In that case, gas pressure may achieve tens Torr, and energy stored in SDO can grow considerably. In the Project, the experimental and theoretical studies of possibilities of gas pressure increase, of an enhancement of SDO yield in conditions of gas flow through the discharge region were carried out. To successfully accomplish this objective, gas flow experimental facilities were developed for modeling of real experimental conditions of electric discharge SDO production system. A new subsonic gas flow RF slab discharge facility with possibilities of gas mixture pre-cooling (before discharge) and electrodes cooling was developed. Parametric study of influence of different parameters on SDO production and transportation in gas flow transverse RF discharge was experimentally carried out. Notable amount of atomic oxygen, which is a strong quencher of SDO, is produced in an electric discharge in oxygen gas mixture. In some papers it was demonstrated that a little NO admixtures resulted in a decrease of atomic oxygen concentration. The effect can be used to decrease SDO losses at transportation of SDO. In the Project, a study of influence of admixtures decreasing atomic oxygen concentration on SDO yield was carried out in a slab repetitively pulsed RF discharge without and with gas flow.

Task B. Possibility study of a technique of compulsory atomic iodine production.

The SDO yields demonstrated in our experiments and observed trends in dependences of this parameter on experimental conditions make it possible to expect that the yield value close to the room temperature threshold level can be obtained. Parameters of the active gas mixture are determined, apart from SDO concentration, by concentration of produced atomic iodine. It is obvious that the electric discharge cannot be used for iodine atoms generation in gas mixtures with SDO yield close to the threshold value, because of great heat release and, hence, active gas mixture heating. The procedure of pulsed volumetric production of atomic iodine was earlier successfully approbated and enables one to produce high concentration of atomic iodine even at low gas pressures and not very high SDO concentration. The active gas mixture was produced by mixing SDO obtained in an electric discharge with an iodine donor, and with subsequent photolytical dissociation of the iodine donor. Products of electric discharge in oxygen can strongly spoil forming of mixture of the iodine donor with SDO produced in the discharge. The search of ways minimizing this effect was also the subject of the Project. Experiments aimed at optimization of active gas mixture parameters were accomplished on the base of study its characteristics in pulsed mode of operation.

Task C. Theoretical modeling of the processes in gas flow containing SDO and iodine mixture.

Quite recently, it was reported that electrically generated SDO yield above threshold value was obtained. These achievements make it reasonable to apply our theoretical model for

evaluation of possibility to realize the electric discharge SDO production system. Generally, conditions adopted in the theory should be a result of compromise between required ideal conditions and that, which can be realized experimentally. Therefore the extension of theoretical model taking into account reactions with iodides and gas dynamic effects in gas flow is of great interest for the complete description of an electric discharge SDO production system and numerical optimization of its parameters. The developed theoretical model was extended by including into it the respective processes.

1.3. Technical Approach and Expected Results.

The study of SDO production in slab RF discharge.

Influence of admixtures decreasing atomic oxygen concentration on SDO yield was studied by stationary (without gas flow) and gas flow slab RF discharge facility. The method is based on detection of SDO luminescence by sensitive photodetector at wavelength of 1.27 μm. A new subsonic gas flow RF slab discharge facility with possibilities of gas mixture pre-cooling (before discharge) and electrodes cooling was developed for modeling of real conditions of electric discharge SDO production system . With this facility, the study of influence of different parameters on SDO production and transportation in gas flow transverse RF discharge was experimentally carried out by method of SDO luminescence detection.

Possibility study of a technique of compulsory atomic iodine production.

From electric discharge SDO generator excited gas was mixed with iodine donor. After the mixing atomic iodine was produced volumetrically by photolysis. Influence of species producing in oxygen discharge plasma on formation of homogeneous mixture of iodine donor and SDO producing in discharge was studied by detection of atomic iodine luminescence at wavelength of 1.315 μm. Optimization of active gas mixture parameters on the base of study its characteristics in pulsed mode of operation was carried out.

Theoretical modeling of the processes in gas flow containing SDO and iodine mixture .

The existing theoretical model was extended by taking into account reactions with iodides and gas dynamic effects in gas flow containing electrically generated SDO and iodine. The model was used for numerical calculation of characteristics of active gas mixture formed in experiments, and for numerical optimization of its parameters.

2. Methods, Experiments, Theory, Results.

2.1. SDO production in pulsed EBSD and slab RF discharge.

These experiments, being carried out both in static conditions and with gas flow, are very important for modeling conditions of real electric discharge singlet delta oxygen (SDO) production systems. Influence of admixtures decreasing atomic oxygen concentration on SDO yield was studied by stationary (without gas flow) EBSD and slab RF discharge facility, and gas flow slab RF discharge facility. The method is based on detection of SDO luminescence by sensitive photodetector at wavelength of 1.27 μm. A new subsonic gas flow RF slab discharge facility with possibilities of gas mixture pre-cooling (before discharge) and electrodes cooling was developed for modeling of real conditions of electric discharge SDO production system. With this facility, the study of influence of different parameters on SDO production and transportation in gas flow transverse RF discharge was experimentally carried out by method of SDO luminescence detection.

2.1.1. SDO production in pulsed EBSD and slab RF discharge without gas flow.

Introduction.

Experiments on studying the influence of nitrogen oxides admixtures scavenging atomic oxygen and decreasing its concentration on SDO production and quenching in repetitively-pulsed slab RF discharge were carried out. The experiments were carried out by using experimental facility without gas flow going through the discharge area. The intensity of SDO luminescence was observed to gradually come down to zero in one–two minutes after switching RF discharge on. The color of the discharge glow changed from gray to pink. Electrical characteristics of the RF discharge and matching conditions for RF generator also changed. The changing electric discharge behavior was related with production of various species, which were not extracted out of discharge zone, and did result in changing of conditions of SDO production. Therefore, it was impossible to correctly measure SDO concentration and compare the results with theory. To study the influence of nitrogen oxides admixtures on SDO production and quenching of SDO in pulsed electric discharge, the modeling experiments were carried out with SDO production in single pulse electron-beam sustained discharge (EBSD) without gas flow. The results of the experiments were compared with theory developed by us. Instead of measurement of SDO luminescence downstream in case of gas flow experiments, one can detect time behavior of SDO luminescence after single pulse excitation of gas mixture which transfers SDO luminescence measurement from space to time domain.

Experimental.

Excitation of oxygen containing gas mixture was carried out by pulsed EBSD by applying EBSD facility described in (*Ionin A.A., 2003; Vagin N.P., 2004, 2006*). EBSD pulse duration was ~0.15 ms. Gas pressure changed from 30 to 60 Torr. Gas mixture CO:O_2:He, into which small amount of NO at partial pressure not higher than 0.2 Torr was added, was used in the experiments. Initial NO concentration in a gas cylinder was higher than 99.85%. It should be pointed out that in gas mixture containing large amount of oxygen, nitric oxide NO can be oxidized into nitrogen dioxide NO_2 through the chemical reaction: $2NO + O_2 \rightarrow 2NO_2$. Therefore, when adding NO, the initial oxygen containing mixture contains both NO and NO_2 molecules. Moreover, these molecules can transform into each other in electric discharge due to plasma-chemical reactions $NO_2 + O \rightarrow NO + O_2$ and $NO + O + M \rightarrow NO_2^* + M$, where O is atomic oxygen that is produced in an electric discharge, M is the third body. In the experiments, the initial amount of gas added from NO gas cylinder is indicated as initial NO fraction. SDO luminescence was detected at the wavelength λ=1.27 μm by a germanium

photodetector. A diffraction monochromator with spectral resolution ~ 10 nm was used for spectral selection of the SDO luminescence (*Vagin N.P., 2004, 2006*). In the experiments, when detecting SDO radiation at the wavelength 1.27 μm in the course of EBSD pulse and just after it, strong luminescence not connected with SDO luminescence was observed (see also (*Vagin N.P., 2004, 2006*)). Thus, when presenting time behavior of SDO luminescence below, its intensity at the beginning of SDO luminescence pulse is not considered. The main attention is paid to the decay of SDO luminescence pulse caused by SDO quenching and diminishing of SDO concentration in gas mixture.

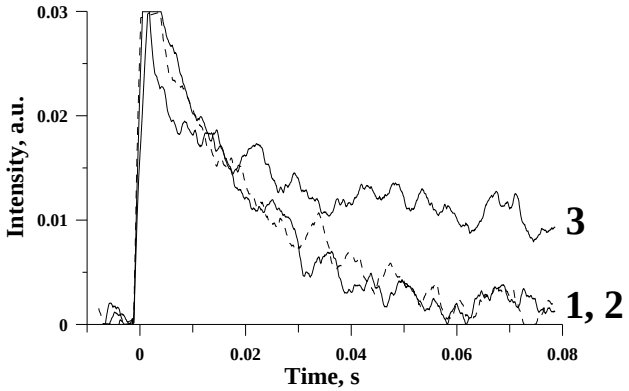

Fig.1. SDO luminescence at the wavelength 1.27 μm. $CO:O_2$=1:19, P=60 Torr.

Initial NO fraction:
1 – 0% (Q_{in}= 160 J/(l atm);
2 – 0.05% (Q_{in}= 160 J/(l atm);
3 – 0.1% (Q_{in}= 130 J/(l atm)

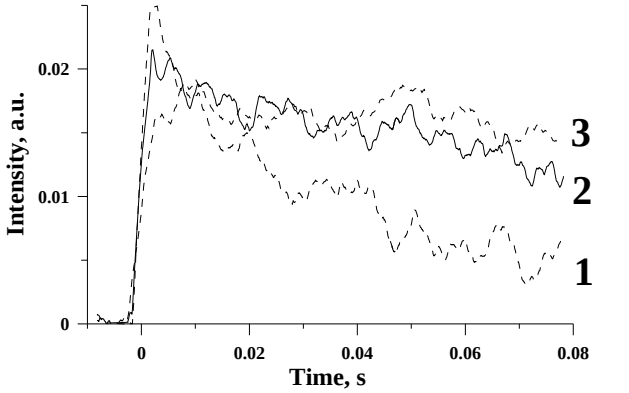

Fig.2. SDO luminescence at the wavelength 1.27 μm. $CO:O_2$=1:49, P= 30 Torr, Q_{in}= 190 J/(l atm)

Initial NO fraction:
1 – 0%,
2 – 0.3%,
3 – 0.7%.

Gas pressure decrease results in enhancement of SDO luminescence pulse duration (compare curves 1 in **Figs.1** and **2**) as in paper (*Vagin N.P., 2006*). However, much more influence on the SDO luminescence is rendered by addition of nitric oxide into oxygen gas mixture (actually, there was a mixture of nitric oxide NO and nitrogen dioxide NO_2). This influence becomes more notable when adding nitric oxide which initial fraction is only 0.1% of oxygen concentration (curve 3 in **Fig.1**). It should be pointed out however, that specific input energy (SIE) Q_{in} for curve 3 in **Fig.1** is almost 20% less than that for curves 1 and 2. Enhancement of initial NO fraction more than 0.3% of oxygen concentration does not practically influence on SDO luminescence pulse duration (curves 2 and 3 in **Fig.2**).

SDO production in electric discharge strongly depends on SIE (*Vagin N.P., 2004, 2006*). Initial nitric oxide addition leads to SIE decrease which is related to conversion of NO into NO_2. For more correct study of NO influence on SDO time behavior, dependences of SDO luminescence intensity on SIE for 10 ms (**Fig.3**) and 80 ms (**Fig.4**) after EBSD pulse at various initial NO fractions were measured. Experimental errors on the figures are mainly due to photodetector noise.

10 ms after EBSD pulse, nitric oxide addition results in insignificant enhancement of SDO luminescence intensity (consequently, SDO concentration) at the same SIE (**Fig.3**). Significant influence of NO addition is observed 80 ms after EBSD pulse (**Fig.4**). Signal/noise ratio in the experiment was close to 1.0 without NO addition, whereas at 0.2% initial NO fraction one can reliably detect SDO luminescence. Similar dependences are observed for helium-free oxygen mixtures at gas pressure from 30 to 60 Torr. It should be pointed out that SDO luminescence intensity decrease at SIE higher than 800 J l^{-1} atm^{-1}($CO+O_2$) is related to gas temperature rise which is accompanied by gas expansion out of electric discharge zone from which SDO signal is detected. Because a ballast volume in the experimental facility was larger than EBSD volume, density of gas mixture including SDO is inversely proportional to gas temperature (see also (*Vagin N.P., 2006*)).

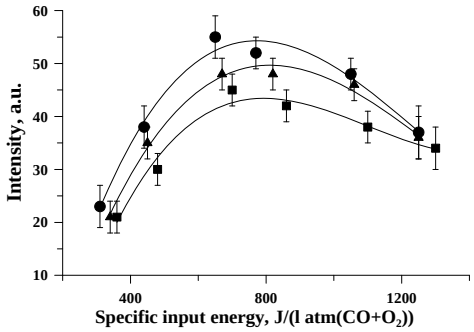

Fig.3. Intensity of SDO luminescence 10 ms after EBSD pulse versus SIE. $CO:O_2$:He=1:19:20, P=60 Torr. Initial NO fraction: ■ - 0%, ▲ - 0.1%, ● - 0.2%.

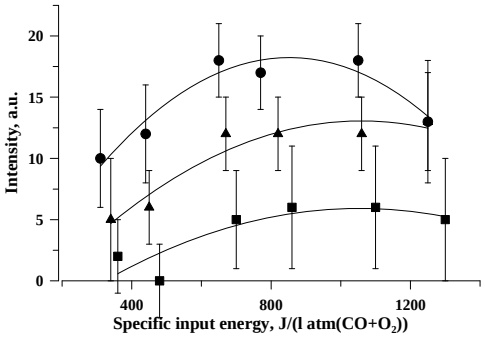

Fig.4. Intensity of SDO luminescence 80 ms after EBSD pulse versus SIE. $CO:O_2$:He=1:19:20, P=60 Torr. Initial NO fraction: ■ - 0%, ▲ - 0.1%, ● - 0.2%.

It was experimentally demonstrated that addition of nitrogen oxide with initial fractions 0.1 – 0.3% of oxygen concentration results in significant enhancement of singled delta oxygen life-time (duration of singled delta oxygen luminescence), which is related to diminishing of atomic oxygen concentration in electric discharge afterglow. It is experimentally shown that at gas pressures 30-60 Torr for getting high singlet delta oxygen concentration on time intervals shorter than ~500 ms one needs to add into oxygen gas mixture nitrogen oxides with fraction not less than 0.2% of oxygen concentration. For intervals longer than ~500 ms one can add 0.1% fraction of nitrogen oxide.

Theoretical.

Kinetic processes with participation of NO и NO_2 molecules were added into the kinetic model previously developed by us for description of self-sustained discharge (*VaginN.P., 2003*) and non-self-sustained (*Ionin A.A., 2003*). In the kinetic model a system of dynamic balance equations for various plasma components including electrons, positive and negative ions, and chemical components O_2; O; O_3; O_2(v); $O_2(a^1\Delta_g)$; $O_2(b^1\Sigma^+_g)$; O_2(4.5); $O(^3P)$; $O(^1D)$; O^+; O_2^+; O_4^+; O^-; O_2^-; O_3^-; CO; CO(v=0, v=1,…v=10); CO^+; He; He(19.8); He^+; He_2^+; NO; NO(v); NO(5.5); NO(7.3); NO^+; $N_2O_2^+$; NO_2; NO_2^- and *e* was being solved. Numerals in brackets designate the energy of respective molecular/atomic states in eV unit. The letter v designates molecular vibrational-rotational states. The other symbols designate electronically excited states. The system of balance equations were solved together with Boltzmann equation in two-term approximation for electron energy distribution function (EEDF). Electron energy losses under elastic collisions with atoms and molecules, excitation of molecular rotational and

vibrational levels, excitation of electronic states, ionization of atoms and molecules, electron attachment to various plasma components were taken into consideration in the Boltzmann equation. Electron collisions with vibrationally and electronically excited molecules were also taken into consideration. To take into account vibrationally excited molecules NO и O_2, an effective vibrational level was introduced for each of these molecules. The multilevel model of vibrational kinetics was developed for CO molecules in the framework of analytical approximation (*Ionin A.A., 2003*). Together with these equations, equations for electrical circuit and equation for translational temperature were solved. Interpolation taking into account a transfer from permanent gas density to permanent gas pressure was carried out in the equation of translational temperature. The terms taking into account gas expansion after a pulsed discharge was added into the balance equations.

The main processes resulting in scavenging atomic oxygen are processes that are chain ones:

$$O + NO + M \rightarrow NO_2 + M, \quad (1)$$

$$O + NO_2 \rightarrow NO + O_2. \quad (2)$$

For high gas pressures (higher than 100 Torr) three-body reaction (1) transforms into two-body reaction with rate constant $3 \cdot 10^{-11}$ $см^3/с$. Apart from processes with participation of neutral atoms and molecules, fast ion-molecular reactions of charge exchange are taken into account:

$$O_2^- + NO_2 \rightarrow NO_2^- + O_2, \quad (3)$$

$$O^- + NO_2 \rightarrow NO_2^- + O. \quad (4)$$

These processes result in formation of ion NO_2^- with energy of electron affinity 2.43 eV that is notably higher than those for O and O_2 - 1.465 and 0.44 eV, respectively. Formation of NO^- was not taken into consideration in the given paper as compared to paper (*Arakoni R.A., 2007*), because of the fact that energy of electron affinity for NO is only 0.031 eV that is close to energy of molecular thermal motion. Addition of NO molecules into gas mixture results in enhancement of electron detachment rate for process:

$$O^- + NO \rightarrow NO_2 + e. \quad (5)$$

In its turn, this reaction leads to enhancement of conductivity of electric discharge plasma.

Fig.5 demonstrates results of numerical calculations of influence of NO и NO_2 fraction on SIE determined for molecular components at the same initial voltage on the capacitor bank. Addition of nitric oxide NO with fraction ~0.4% of full gas pressure led to insignificant SIE increase, whereas nitrogen dioxide NO_2 admixture resulted in substantial SIE decrease. The latter SIE decrease is related to formation of negative ion NO_2^-. The former small SIE increase, when adding NO molecules at partial gas pressure higher than 0.02% of full pressure, is connected with charge exchange of ions O_2^+ accompanied by formation of ions NO^+ which unlike ions O_2^+, are not transformed into ions with faster recombination rate, and with reaction (5).

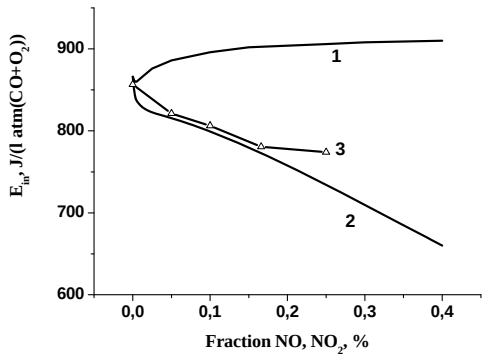

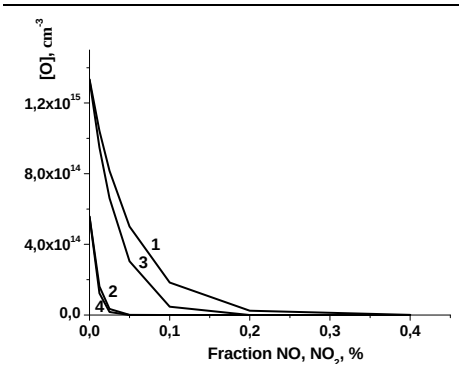

Fig.5. Theoretical (**1,2**) and experimental (**3**) dependencies of SIE on fraction of nitrogen oxides in gas mixture He:O_2:CO =20:19:1 for NO (**1,3**) and NO_2 (**2**).
Gas pressure = 60 Torr;
initial voltage U_0 = 2.5 kV

Fig.6. Calculated atomic oxygen O concentration versus fractions of NO (curves **1, 2**) and NO_2 (curves **3, 4**) 10 ms (**1, 3**) and 80 ms (**2, 4**) after the beginning of EBSD pulse. He:O_2:CO =20:19:1, P = 60 Torr, U_0 = 2.8 kV. NO and NO_2 fractions were determined of full gas pressure.

Fig.6 demonstrates calculated dependence of concentration of atomic oxygen produced in electric discharge due to molecular oxygen O_2 dissociation under electron collisions on fractions of NO *и* NO_2 molecules 10 and 80 ms after the beginning of EBSD pulse. It follows from the figure that NO_2 molecules scavenge atomic oxygen more effectively than NO molecules.

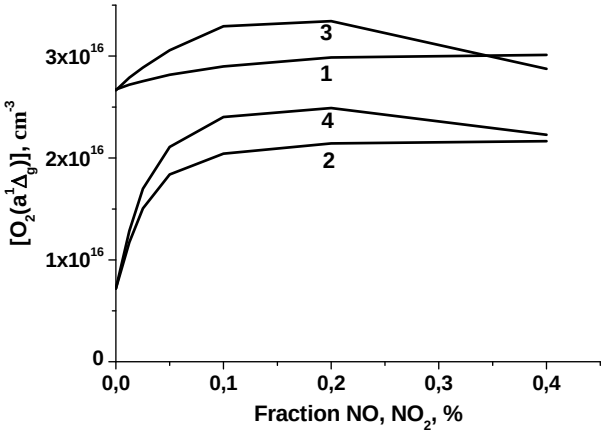

Fig.7. Calculated dependences of SDO concentration on NO (curves **1, 2**) and NO_2 (curves **3, 4**) fraction for different moments of time 10 ms (**1,3**) and 80 ms (**2,4**). He:O_2:CO =20:19:1, P = 60 Torr, U_0 = 2.8 kV. NO and NO_2 fractions were determined of full gas pressure

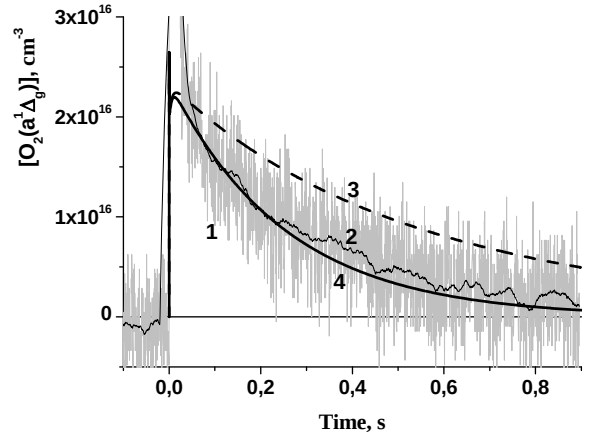

Fig.8. Comparison of experimental and calculated time behavior of $O_2(a^1\Delta_g)$ relaxation. **1** – photodetector signal; **2** – signal 1 averaged over 100 points; **3** – calculation with relaxation rate constants of $O_2(a^1\Delta_g)$ quenching by O_2 taken from *(Eliasson B., Kogelschatz U., 1986)*; **4** – with relaxation constants estimated in the given paper. He:O_2:CO:NO_2 =20:19:1:0.04, P = 60 Torr, U_0 = 2.4 kV.

Fig.7. presents calculated dependences of SDO concentration on NO and NO_2 fractions for two moments of time 10 and 80 ms. When adding nitrogen oxides, the change of SDO concentration for short time interval 10 ms is not very high, whereas for longer time interval 80 ms small amount (~0.1%) of nitrogen oxides results in several times enhancement of SDO concentration.

Comparison of experimental and calculated time behavior of SDO concentration is presented in **Fig.8** that demonstrates a photodetector signal of SDO luminescence, the same signal averaged over 100 points, and results of calculations. The experimental dependence of relative SDO concentration is normalized by calculated SDO concentration. The dotted line is

obtained by using approximation from (*Eliasson B., Kogelschatz U., 1986*). The solid line is obtained by using relaxation constants estimated in the given paper.

Conclusion.

Experimental and theoretical studies are performed on influence of nitrogen oxides (NO and NO_2) on the specific energy input in a pulsed e-beam sustained discharge. Theory predicts that addition of NO results in an insignificant increase of the energy input, while addition of NO_2 leads to its decrease. The last case is explained by a higher electron affinity for NO_2 molecule. Experiment and theory demonstrate that addition of nitrogen oxides in an amount 0.1 – 0.3 % leads to a remarkable reduction of atomic oxygen concentration in the afterglow.

Using $O_2(a^1\Delta_g)$ luminescence measurements, the temperature dependence of $O_2(a^1\Delta_g)$ relaxation in collisions with O_2 molecules was determined.

At gas pressures within (30 – 60) Torr the acceptable SDO concentration can be achieved at times shorter 0.5 s, if nitrogen oxides are added in an amount not less than 0.2% of oxygen molecules.

2.1.2. SDO production in slab RF discharge with gas flow.

Introduction.

One of promising types of gas discharge generators of singlet oxygen is the capacitive coupled RF slab discharge with fast gas flow. It allows for achieving the required level of SDO concentration and effective cooling of gas flow through the electrodes. To do a theoretical prognosis of available SDO production efficiency, the respective numerical model should be developed.

Pulse-periodic mode of operation of the RF discharge provides new options for managing SDO generation. In this case, the gas plug transporting through the discharge zone experienced the repeated action of the discharge. The number of discharge pulses exciting this plug is a function of the repetition frequency, and the average discharge power depends on pulse power and duty cycle of RF discharge pulses. Further modification of the model is necessary to describe such a system.

Technical.

For further experiments an electric discharge chamber, which was previously used as a part of a pulsed supersonic e-beam sustained discharge CO laser (**Figs.9 and 10**) was modified to have a possibility of carrying out modeling experiments on SDO production in transverse RF discharge ignited in subsonic gas flow.

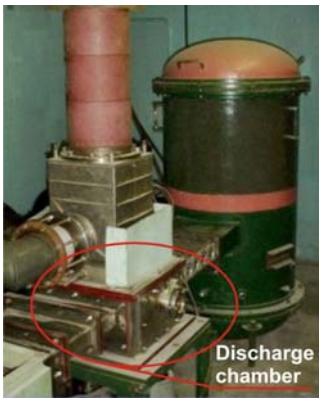

Fig.9. Pulsed supersonic e-beam sustained discharge CO laser design.

Fig.10. Modified discharge chamber.

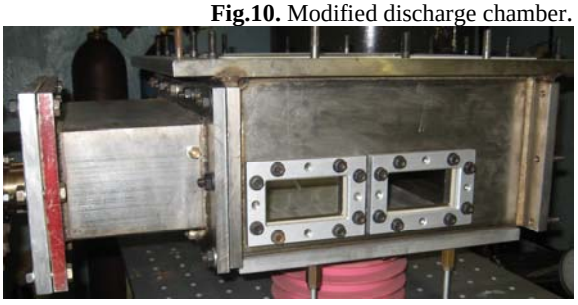

The discharge chamber modification was made according to a concept simplified view of which is presented in **Fig.11.**

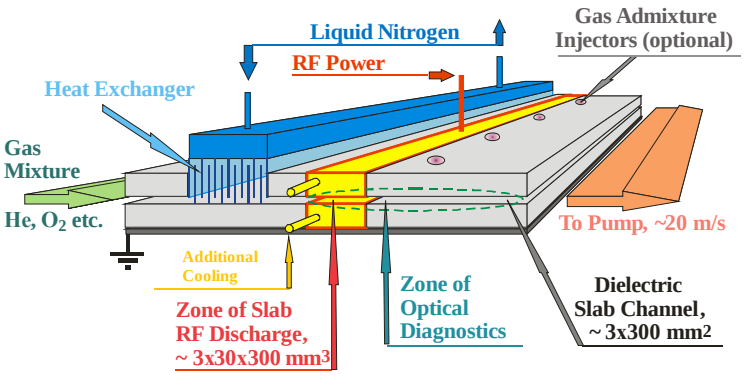

Fig.11. A concept of the experimental setup.

The following items were developed and put into the chamber: gas flow duct including multi-path cryogenic heat exchanger (**Fig.12a**) for preliminary gas cooling (down to ~100-120K), dielectric slab channel (**Fig.12b**) of ~3x300 mm^2 cross section for gas flow formation, and slab electrode system (**Fig.12c**) (with possible additional cooling) incorporated in the channel downstream from the heat exchanger for RF discharge ignition.

a **b** **c**

Fig.12. Parts of the gas flow duct inside modified discharge chamber. **a** - heat exchanger, **b** - dielectric slab channel, **c** - RF discharge electrode system.

Vacuum pumps of total productivity ~20 liter/s at gas pressure up to ~50 Torr were connected to one side of the discharge chamber using two flexible tubes for supplying stationary gas flow rate (up to ~20 m/s) through the RF discharge channel. The tube from a gas mixture preparing and supplying system was connected to the other side of the gas flow duct. An upper and two side covers of the chamber were also modified. The side covers were supplied with optical windows (**Fig.13**) for singlet delta oxygen luminescence observation at different points of the gas flow downstream of RF discharge zone. Additional vacuum and electrical leads-in (**Fig.13**) were also arranged in side covers for diagnostics and monitoring system.

Fig.13. Optical window and additional vacuum and electrical leads-in at side cover of the chamber.

Fig.14. RF power supply. 500 W, 81 MHz.

The design of the upper cover was developed by adding four thermo-isolated leads-in for supplying of the liquid nitrogen to the heat exchanger and two electrically-isolated leads-in to connect RF electrode system with external RF power supply (**Fig.14**).

All internal parts of the facility (cryogenic heat exchanger, dielectric slit channel, RF discharge electrode system, glass side walls forming the gas flow) were coupled to each other and tested for the operation. First experiments on SDO production in transverse gas flow RF discharge were carried out for pure oxygen with electrode system cooled by room temperature water (without cryogenic gas pre-cooling). The scheme of the SDO luminescence registration experiments is presented in **Fig.15**.

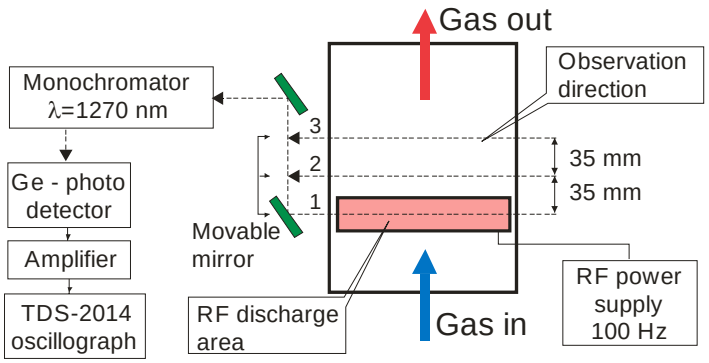

Fig.15. The scheme of SDO luminescence observation in transverse gas flow excited by repetitively pulsed RF discharge.

Experimental (repetitively pulsed mode).

The first series of the experiments was performed with 12 Torr pure O_2 gas flowing through the RF discharge zone at very low velocity (near the minimum of not controlled value). RF power supply (working frequency 81.36 MHz) operated at ~620 W power modulated by 100 Hz pulse repetition rate with RF power pulse width from 0.2 ms up to 1 ms. Path #1 (see **Fig.16**) was used for SDO luminescence observation in these experiments. For these conditions SDO luminescence intensity time behavior depending on the RF power pulse width is presented in **Fig.16.**

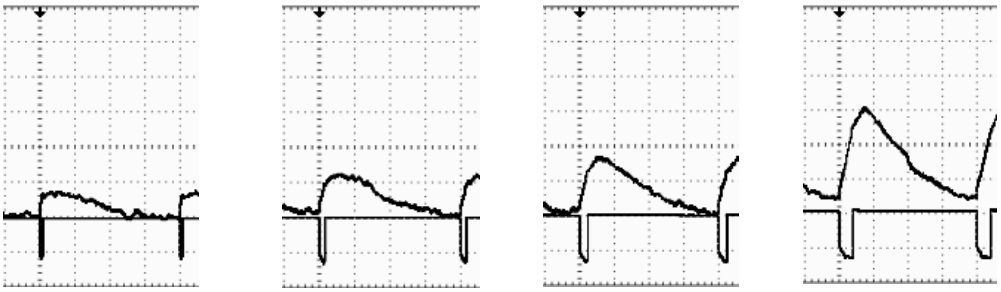

a **b** **c** **d**

Fig.16. SDO luminescence intensity time behavior (upper trace) and RF pump pulses (lower trace, inverted). Pure O_2, 12 Torr. Observation path #1. RF power pulse width - 0.2 ms (a), 0.4 ms (b), 0.6 ms (c), and 1.0 ms (d). Time scale 2.5 ms/div.

It should be noted that the "zero"-level for the upper traces in **Fig.16** (and in all following oscilloscope traces) coincided with horizontal parts of lower traces. Thus, the residual SDO

concentration left of the previous pump pulse can be seen at the beginning of the pump pulse (**Fig.16d**). The same measurements were carried out for pure O_2 gas flow at gas pressure of 25 Torr (**Fig.17**). The RF discharge and gas flow parameters were as the same as for the previous series.

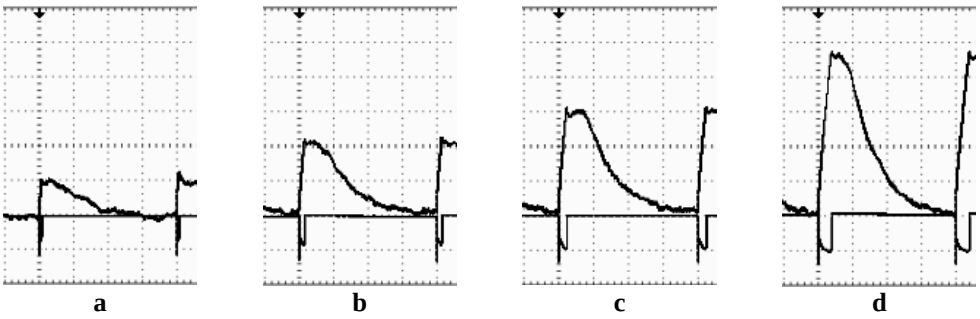

Fig.17. SDO luminescence intensity time behavior (upper trace) and RF pump pulses (lower trace, inverted). Pure O_2, 25 Torr. Observation path #1. RF power pulse width - 0.2 ms (a), 0.4 ms (b), 0.6 ms (c), and 1.0 ms (d). Time scale 2.5 ms/div.

One can see from **Figs.16** and **17** that the amplitude of SDO luminescence became higher for higher pressure of the excited gas. Simultaneously, the SDO life time was about twice less (compare FWHM of luminescence intensity pulses in corresponding **Figs.16** and **17**). Moreover, one can see from these figures that the higher the energy loaded into the RF discharge is, the higher is the maximum SDO yield that is about linear proportional to this energy (or pump pulse width at fixed pump power).

To be sure that the observed signals represented just SDO luminescence, spectral line profile was measured by tuning of working wavelength of the monochromator. The luminescence signals corresponding to the fifth millisecond in afterglow of the RF discharge pulse (**Fig.18**) were chosen for spectral line profile calculations to avoid the influence of light emitting from the discharge zone during the excitation pulse (see, for example, **Figs.18d** and **18e**).

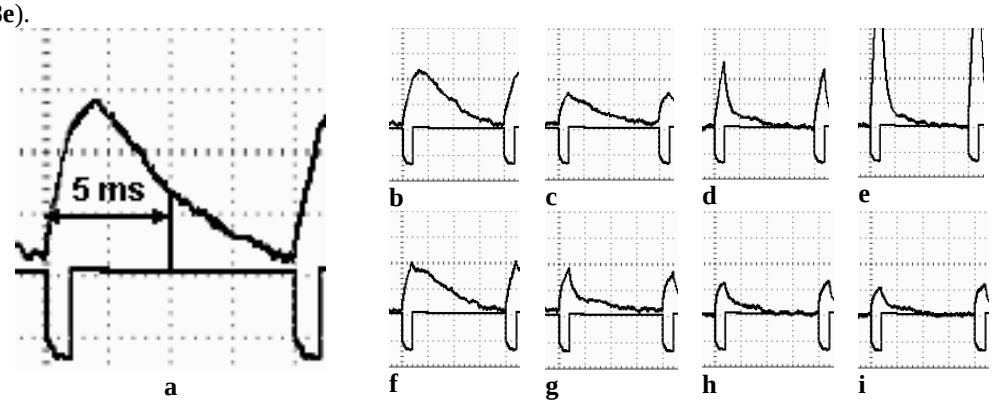

Fig.18. SDO luminescence intensity time behavior (upper trace) and RF pump pulses (lower trace, inverted). Pure O_2, 12 Torr. Observation path #1. RF power pulse width - 1.0 ms. Monochromator wavelength λ=(1270+X) nm. X=0 (a), 11 (b), 22 (c), 33 (d), 44 (e).
X=-11 (f), -22 (g), -33 (h), and -44 (i). Time scale 2.5 ms/div.

For the conditions of **Fig.18** the spectral line profile corresponding to the fifth millisecond of RF discharge pulse afterglow is presented in **Fig.19**.

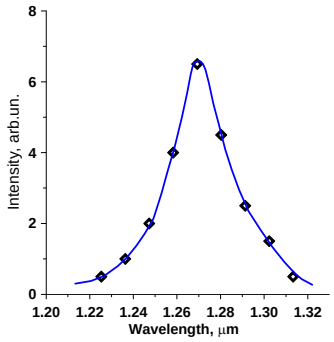

Fig.19. SDO spectral line profile corresponding to the fifth millisecond of RF discharge pulse afterglow.

The next series of the experiments (**Fig.20**) was performed for different pure O_2 flow rates through the RF discharge zone, and SDO luminescence was observed from different zones downstream of the discharge zone (see **Fig.15**). The conditions of all these experiments were the same: gas pressure in the discharge channel 12 Torr, electrode system cooled by water, RF pump pulse repetition rate 100 Hz, RF pulse duration 1 ms, RF pulse power 620 W.

Looking at the traces presented in **Fig.20**, real gas flow rate may be calculated using vertical columns corresponding to constant gas flow rate (for example, $V=V_{max}$ or $V=V_{max}/2$). Identifying the time positions of the SDO intensity maxima with real geometry of the luminescence observations, V_{max} appeared to be equal about 35-40 m/s (in conditions of the experiments presented above).

Fig.20. SDO luminescence signals for different pure O_2 flow rates (from $V=V_{max}$ down to $V=0$) observed from different zones downstream of the discharge area (observation pathes #1, #2, and #3). Time scale 2.5 ms/div, vertical scale - constant. The negative peak in the SDO signal during the pump pulse is an electrical interference.

Also, reference trace in static conditions corresponding to V=0 through the observation path #1 was produced for further calibration of the measurement system using results (namely SDO yield estimations) of our previous research (*Ionin A.A., 2007a*)

Theoretical (repetitively pulsed mode).

Developed earlier by us kinetic models (*Ionin A.A., 2007b*) for description of self-sustained and electron-beam sustained discharges in oxygen-containing mixtures and their extension to addition of NO and NO_2 molecules (*Ionin A.A., 2009a*) were modified to do studies on pulse periodic transverse flow RF discharge.

An approximation of plug-flow model is implemented where evolution of plasma components while transporting in a channel is calculated as evolution in time. The gas flow velocity in calculations was taken equal to 30 m/s.

Fig. 21 demonstrates values of elastic and inelastic collision frequencies as functions of *E*/N parameter (*E* is an amplitude of the electric field strength, *N* is current gas density) in comparison with the RF angular frequency. It is seen that for experimental conditions (dashed zone in **Fig. 21**) the inelastic collision frequency is higher than the RF frequency. It was shown in (*Dyatko N.A., 1985*) that at this condition the constant electric field approximation can be employed.

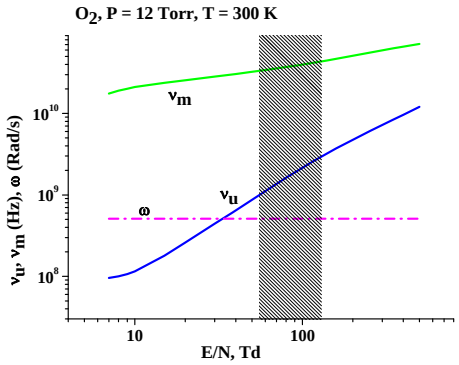

Fig. 21. Elastic (ν_m) and inelastic (ν_u) collision frequencies vs E/N for oxygen with pressure 12 Torr. Dash-dot line is for RF angular frequency, ω. Dashed zone indicates variation range of *E*/*N* amplitude in numerical simulations.

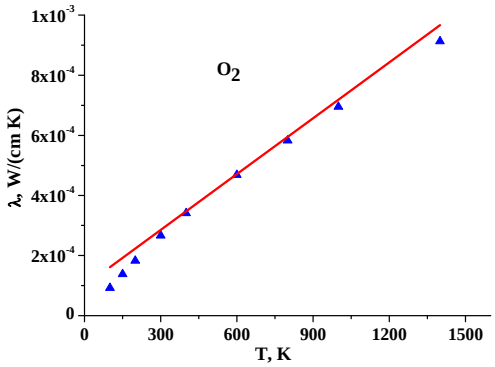

Fig. 22. Thermal conduction coefficient for O_2 molecules as a function of gas temperature. Triangles are data from (*Grigoriev I.S., 1991*), line is our linear interpolation.

In the experiments the water cooled aluminum electrodes were separated by the gap of 3 mm, the gas residence time at the maximal flow velocity 30 m/s is equal to 1 ms. Then the thermal conductivity leads to a remarkable reduction of gas heating. To take into account this process the respective term was added into the gas thermal balance equation:

$$C_V kN \frac{dT}{dt} = P_{HEATING} + kT\frac{dN}{dt} - \frac{\lambda}{\Lambda^2}(T - T_0), \qquad (6)$$

where λ is the thermal conduction coefficient; C_V is the constant volume thermal capacity; κ is the Boltzmann constant; N is the gas density; $\Lambda^2 = \left(\frac{d}{\pi}\right)^2$; $P_{HEATING}$ the heating power density in the discharge and after its termination. The second term in the right-hand part of the equation accounts for gas expansion and the third one for thermal cooling. It was assumed that the temperature of electrodes is kept constant equal to the temperature of cooling water T_0. We

used in calculations the linear approximation for temperature dependence of the thermal conduction coefficient (**Fig.22**).

Acoustic wave transit time estimated by formula $\tau_s = \frac{a}{2u_s}$ (a is the discharge size along the flow), is about 50 μs. At times shorter than τ_s the gas density was taken as a constant, while at much longer times the pressure was set constant. At intermediate times the gas density was approximated by a formula:

$$N(t) = N_0 e^{-\frac{t}{\tau_s}} + N_0 \frac{T_{t=0}}{T}(1 - e^{-\frac{t}{\tau_s}}) \qquad (7)$$

where N_0 and $T_{t=0}$ are initial gas density and temperature. In kinetic equations for plasma components the respective terms were introduced, which reflect influence of gas expansion. This approach was formulated earlier in Ref. (*Akishev Yu.S., 1982*).

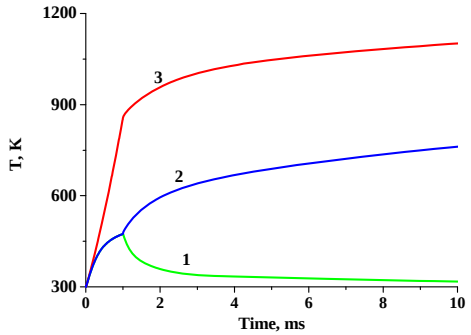

Fig. 23. The gas temperature time behavior. 1 - thermal conduction cooling is accounted for in all channel; 2 – thermal conduction is accounted for in the discharge zone only; 3 - thermal conduction is neglected. Pure O_2, P = 12 Tor.

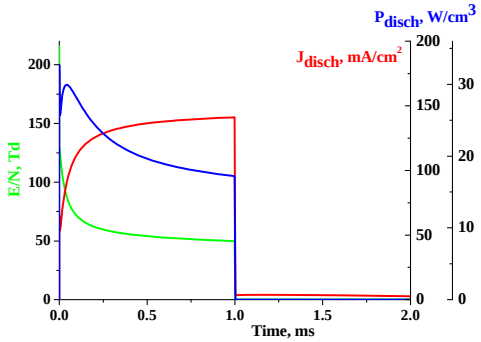

Fig. 24. *E*/*N*, electric current density and discharge power density as functions of time for pure oxygen. P = 12 Torr, initial temperature $T_{t=0}$ = 300 K, thermal cooling is included.

The simplest electric circuit composed of a voltage supply, discharge and ballast resistor was taken in simulations The values of the voltage applied and ballast resistor were found from condition of calculated power density being close to the experimental one.

Fig.23 shows gas temperature evolution for different assumptions about thermal cooling of gas in the channel. Curve 1 is for the case of the fixed wall temperature and the thermal conduction taken into account as described above. Actually, the electrodes are cooled by water (thermal conductivity of aluminum is 2.37 W/cm·K. The walls of the channel in the down flow zone are made from Teflon, which has much lower thermal conductivity $2.3 \cdot 10^{-3}$ W/cm·K. Curve 2 is for calculations when thermal loss through the Teflon walls are neglected. Curve 3 is for the case when no thermal loss was included in the model. One can see that thermal conduction leads to rather strong gas cooling.

Figs.24, 25 show time behavior of discharge characteristics: the reduced electric field strength, the current and power densities. The data in **Fig.24** and **Fig.25** are the same, and figures differ by time scale, linear and logarithmic, respectively. It is worth to note that the discharge characteristics are not sensitive to variations in thermal cooling regimes. The average power density in calculations 21 W/cm^3 is close to the experimental value 23 W/cm^3.

Fig.25 demonstrate that just after breakdown fast reduction of the electric field is stopped on time scale about 1 μs with characteristic value about 130 Td. Then it continues to fall down on a time scale of hundreds of microseconds approaching value about 60-50 Td,

which varies slowly till the end of RF pulse. The first stabilization of *E*/*N* value (130 Td) is due to equilibration of ionization and attachment processes in oxygen. Further reduction of *E*/*N* is caused by accumulation of species: O, $O_2(a^1\Delta_g)$, $O_2(b^1\Sigma^+_g)$. These species effectively destroy negative O^- ions in the following reactions:

$$O^- + O \rightarrow O_2 + e, \quad (8)$$

$$O^- + O_2(a^1\Delta_g) \rightarrow O_3 + e, \quad (9)$$

$$O^- + O_2(b^1\Sigma^+_g) \rightarrow O + O_2 + e, \quad (10)$$

which proceed with rate constants $1.9\cdot10^{-10}$, $3\cdot10^{-10}$ and $7\cdot10^{-10}$ см^3/с, respectively.

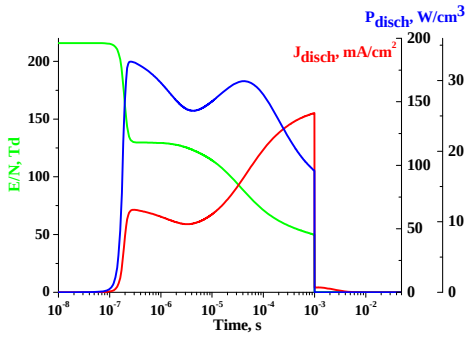

Fig. 25. *E*/*N*, electric current density and discharge power density as functions of time, logarithmic scale of time, data are the same as in **Fig. 24**.

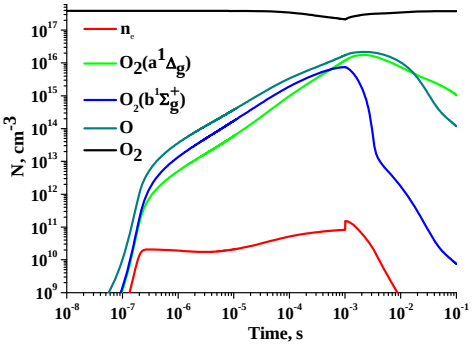

Fig. 26. Time evolution of some plasma components, conditions are as in **Fig. 24.**

Time behavior of some plasma components is shown in **Fig.26**. It is seen that O atom concentration is slightly higher than that of $O_2(a^1\Delta_g)$.

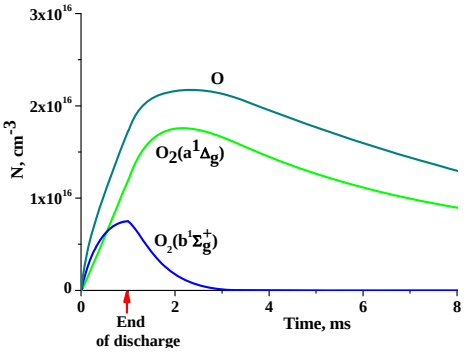

Fig.27. Time evolution of O, $O_2(a^1\Delta_g)$, $O_2(b^1\Sigma^+_g)$ as in **Fig.26**, linear scales of time and number densities. Y = 5.5% at 1 ms, Y = 6.8% at 2.3 ms.

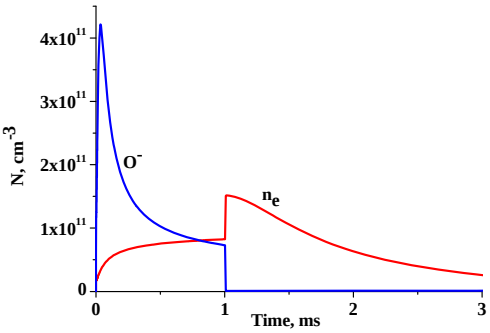

Fig.28. Time evolution of electron and O^- number densities for conditions of **Fig.24**.

Fig.27 demonstrates time evolution of O, $O_2(a^1\Delta_g)$, $O_2(b^1\Sigma^+_g)$. At the moment of RF discharge termination the yield of $O_2(a^1\Delta_g)$ amounts 5.5%. The SDO yield approaches maximum in the afterglow at the moment 2.3 ms and amounts 6.8%.

Electron number density in **Fig.28** grows stepwise 1.8 times at the moment of the voltage switching off. This effect is explained by a fast drop of electron temperature in the absence of the electric field and followed reduction of the dissociative attachment rate, which was compensated in the discharge by detachment processes (8)-(10). As a result, these processes serve as a strong source of electrons. After disappearance of O^- the decay of plasma continues due to recombination processes.

Experimental (CW mode).

The influence of gas mixture parameters (gas pressure, content, and flow rate) and the value of RF power loaded into discharge (and the low frequency modulation parameters) on the SDO production in slab RF discharge were studied in the following experimental series. SDO luminescence registration was carried out using optical scheme presented in **Fig.15**. Observation path #3 (see **Fig.15)** 70 mm downstream off the center of the RF discharge zone was used in the experiments.

In most experiments described below RF power supply operated in CW mode. For this reason, an optical modulator (mechanically rotating disk with slits, modulation rate ~50 Hz) was inserted into the path of luminescence observation in front of the input slit of the monochromator to have the possibility of week signals accumulation and noise reduction. To be sure that the observed signal was really the SDO luminescence, its spectral distribution was measured in each series of the experiments. In all cases the distribution was identical to one presented in **Fig.19.**

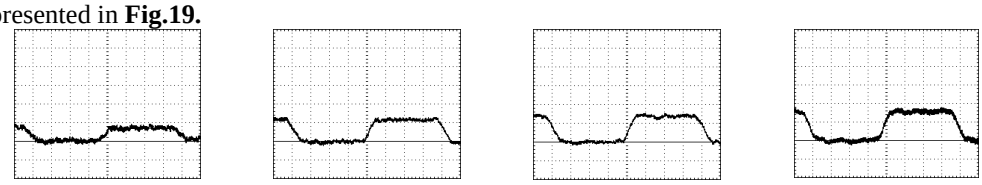

Fig.29. SDO luminescence intensity. P=7.5 Torr, CW RF power 100 W (a), 200 W (b), 300 W (c), and 400 W (d). Pure O_2. Time scale 2.5 ms/div.

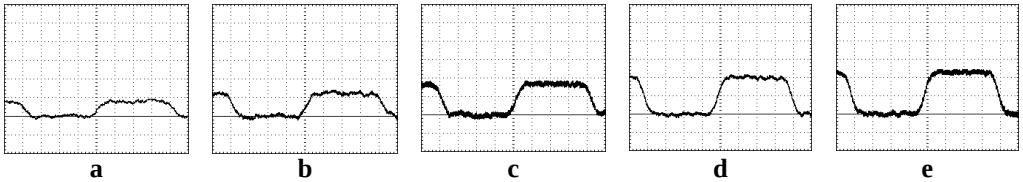

Fig.30. SDO luminescence intensity. P=15 Torr, CW RF power 100 W (a), 200 W (b), 300 W (c), 400 W (d), and 500 W (e). Pure O_2.Time scale 2.5 ms/div.

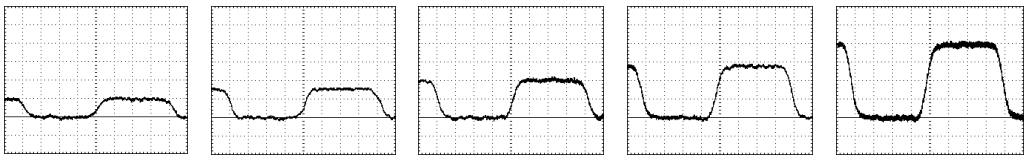

Fig.31. SDO luminescence intensity. P=30 Torr, CW RF power 100 W (a), 200 W (b), 300 W (c), 500 W (d), and 700 W (e). Pure O_2. Time scale 2.5 ms/div.

SDO luminescence intensity signals (modulated with 50 Hz optical chopper) obtained in pure oxygen at different gas pressures excited by CW RF discharge of different power are presented in **Figs.29-31**. Gas flow rate in these experiments was maximal ($V=V_{max}$) and equal to ~30 m/s. The increase of RF power loaded into the discharge leaded to an increase of SDO

luminescence intensity. For more convenient analysis of the results obtained, the data from **Figs.29-31** were recalculated (see **Figs.32-35**) by the following way. In these figures X-axis represents either CW RF power (P_{in}) or specific input energy (SIE) loaded into discharge. (In conditions of the experiments with gas flow, space scaling along flow direction with CW excitation is to some extent equivalent to time scaling in static conditions with single pulse RF discharge excitation. In the latter case the pulse duration is defined by the time needed for the gas to flow through the discharge zone. In the experiments with $V=V_{max}$ this time was ~1 ms.) Y-axis in **Figs.32-35** represents either observed SDO luminescence intensity (which is proportional to the SDO concentration) or specific intensity normalized to the partial O_2 pressure (which is proportional to SDO yield).

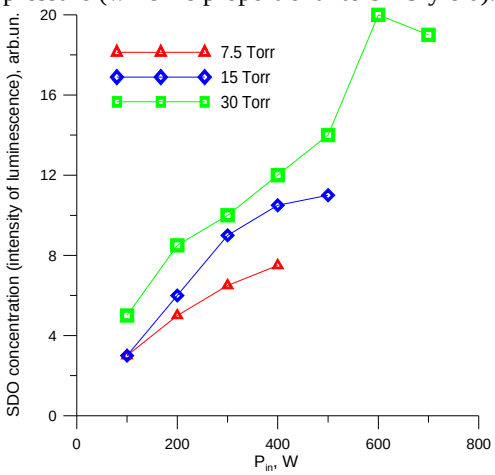

Fig.32. SDO concentration (luminescence intensity) vs. RF power P_{in} loaded into discharge. Pure O_2, pressure 7.5, 15, and 30 Torr.

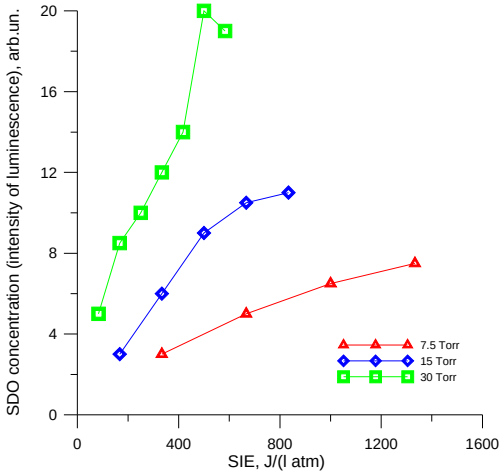

Fig.33. SDO concentration (luminescence intensity) vs. SIE. Pure O_2, pressure 7.5, 15, and 30 Torr.

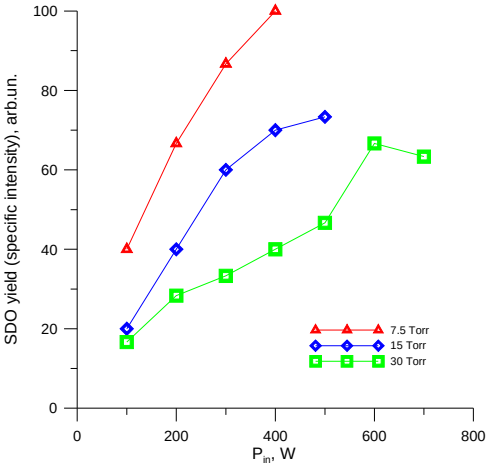

Fig.34. Specific SDO luminescence intensity (normalized to the partial O_2 pressure (which is proportional to the SDO yield). vs. RF power P_{in} loaded into discharge. Pure O_2, pressure 7.5, 15, and 30 Torr.

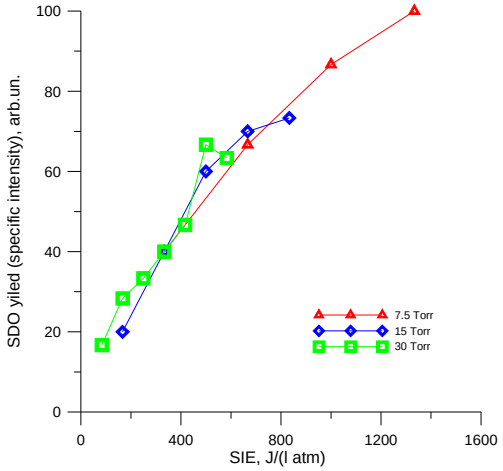

Fig.35. Specific SDO luminescence intensity intensity (normalized to the partial O_2 pressure (which is proportional to the SDO yield) vs. SIE. Pure O_2, pressure 7.5, 15, and 30 Torr.

An increase of pure oxygen pressure resulted in significant increase of SDO concentration (SDO luminescence intensity). It can be especially clearly seen in **Fig.33** where SDO concentration was significantly higher at higher gas pressure just at lower SIE. Concerning SDO yield, another situation was observed: specific luminescence intensity (i.e SDO yield) increased with the decrease of gas pressure at the same RF power loaded into the discharge (see **Fig.34**). In addition, for given experimental conditions (gas flow rate, gas pressure range, gas flight time from discharge zone to the observation zone, etc.) SDO yield depended mainly on SIE but almost not on gas pressure (see **Fig.35**). For it was easier to provide high SIE at low gas pressure, the greatest value of SDO yield in these experiments was realized at gas pressure 7.5 Torr.

The same series of the experiments was carried out for diminished gas flow rate V= $V_{max}/2$=15 m/s. Time traces of SDO luminescence intensity are presented in **Figs.36-38**.

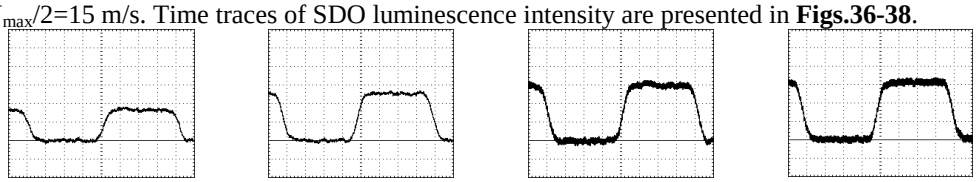

a **b** **c** **d**

Fig.36. SDO luminescence intensity. P=7.5 Torr, CW RF power 100 W (a), 200 W (b), 300 W (c), and 400 W (d). Pure O_2. Time scale 2.5 ms/div. V=$V_{max}/2$.

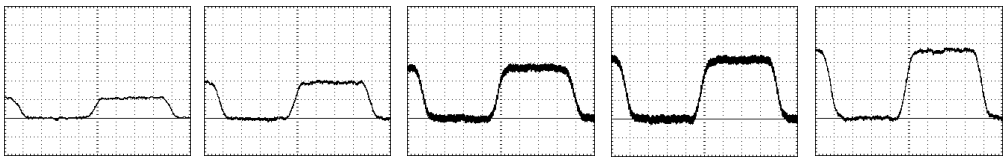

a **b** **c** **d** **e**

Fig.37. SDO luminescence intensity. P=15 Torr, CW RF power 100 W (a), 200 W (b), 300 W (c), 400 W (d), and 500 W (e). Pure O_2.Time scale 2.5 ms/div. V=$V_{max}/2$.

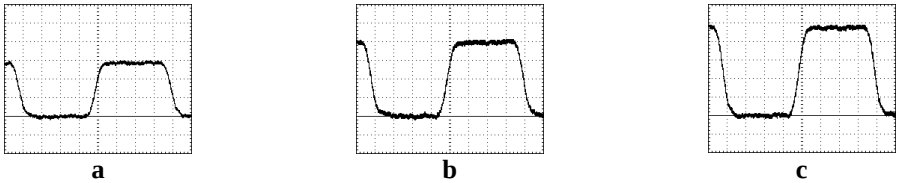

a **b** **c**

Fig.38. SDO luminescence intensity. P=30 Torr, CW RF power 200 W (a), 400 W (b), and 600 W (c). Pure O_2.Time scale 2.5 ms/div. V=$V_{max}/2$.

As compared to previous series (at V=V_{max}), maximal value of SDO concentration observed in the experiments with V=$V_{max}/2$ at gas pressure 7.5 Torr increased about two times. For gas pressure 30 Torr the increase was only 10-15% (compare, for example, **Figs.32, 33** and **Figs.39, 40,** arbitrary units are the same for **Figs. 32, 39,** and **Figs. 33 ,40**).

It should be noted that in the experiments with V=$V_{max}/2$ the time needed for the gas to flow through the discharge zone and to flow from discharge zone to the observation zone was about as twice longer as in case V=V_{max}. It resulted in the increase of SIE and in enlargement of the role of relaxation processes, respectively. At increased gas pressures the rates of three-body reactions (for example, the reaction of SDO quenching: $O_2(^1\Delta_g)+O_2+O\rightarrow O_2+O_2+O$) became significantly higher and it might lead to the decreased SDO concentration observed at higher gas pressures. It can be clearly seen in **Fig.42** where the dependence of specific SDO luminescence intensity (i.e. SDO yield) versus SIE is presented for different gas pressures. Contrary to **Fig.35** where all experimental points are lying at one curve, SDO yield in **Fig.42** is

higher for gas pressure of 7.5 Torr as compared to higher pressures in the whole range of SIE. Also, it should be noted that for all dependencies presented in **Fig.42** (for all gas pressures), the higher the SIE, the smaller the angle of curve inclination. In other words, there is the SDO yield saturation during the increase of SIE. The maximal SDO yield was observed at gas pressure 7.5 Torr and it was about twice as higher as in previous experimental series (compare, for example, **Fig.35** and **Fig.42**).

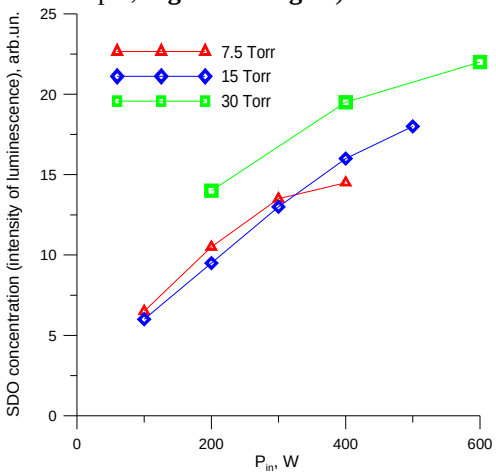

Fig.39. SDO concentration (luminescence intensity) vs. RF power P_{in} loaded into discharge. Pure O_2, pressure 7.5, 15, and 30 Torr. $V=V_{max}/2$.

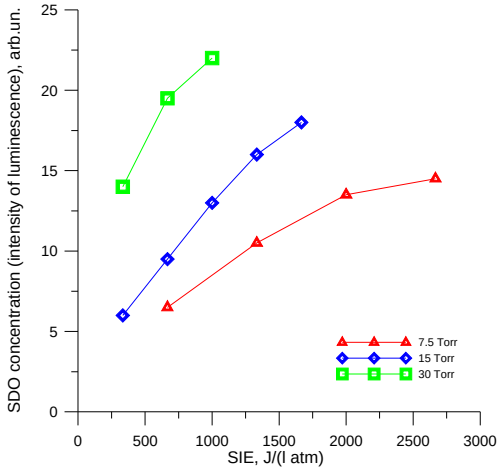

Fig.40. SDO concentration (luminescence intensity) vs. SIE. Pure O_2, pressure 7.5, 15, and 30 Torr. $V=V_{max}/2$.

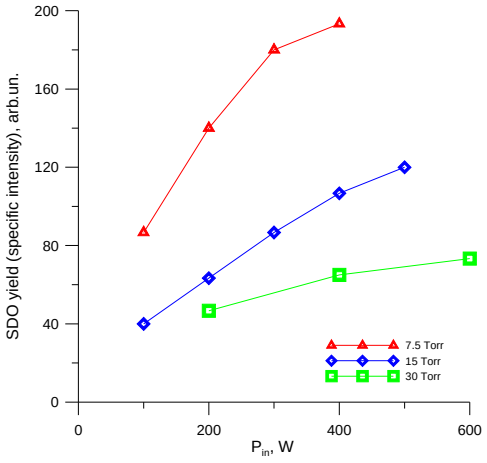

Fig.41. Specific SDO luminescence intensity vs. RF power P_{in} loaded into discharge. Pure O_2, pressure 7.5, 15, and 30 Torr. $V=V_{max}/2$.

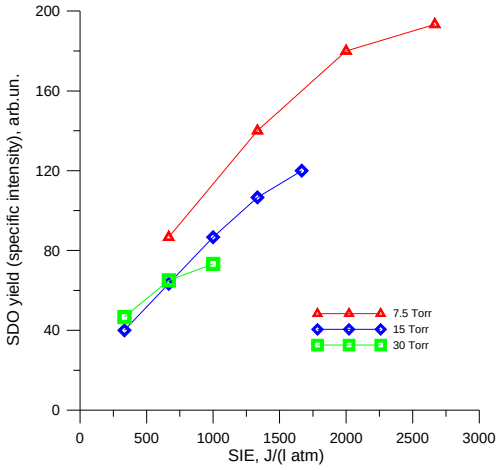

Fig.42. Specific SDO luminescence intensity vs. SIE. Pure O_2, pressure 7.5, 15, and 30 Torr. $V=V_{max}/2$.

In the next series of the experiments SDO production was studied in helium-contained gas mixtures flowing through the RF discharge zone at $V=V_{max}=30$ m/s. The obtained dependencies of SDO concentration vs. RF power loaded into discharge and vs. SIE are presented in **Figs.43** and **44** respectively. Partial pressure of oxygen was constant (7.5 Torr) during the whole series. So, in the experiments, SDO yield (defined as the ratio of SDO luminescence intensity to O_2 partial pressure) was proportional to the SDO luminescence

intensity. An addition of He to pure oxygen resulted in significant (about twice) increase of SDO concentration (and SDO yield, respectively). It should be noted that strong saturation of SDO luminescence with the SIE increase was observed for helium-containing gas mixtures (see **Fig.44**).

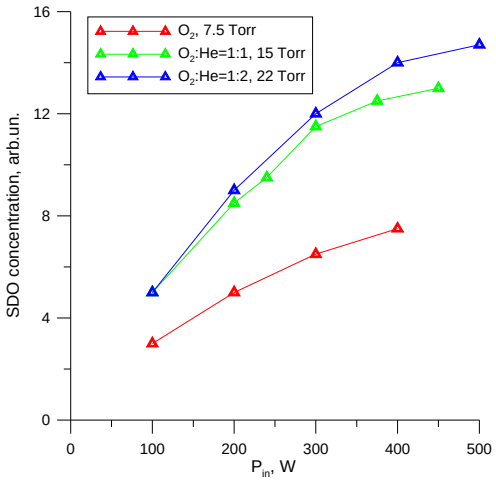

Fig.43. SDO concentration (luminescence intensity) vs. RF power P_{in} loaded into discharge. O_2:He=1:0, 1:1, 1:2; oxygen partial pressure 7.5 Torr; $V=V_{max}$.

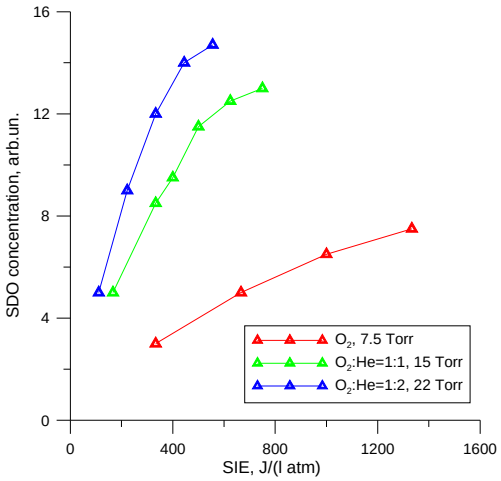

Fig.44. SDO concentration (luminescence intensity) vs. SIE. O_2:He=1:0, 1:1, 1:2; oxygen partial pressure 7.5 Torr; $V=V_{max}$.

It was noted in some publications elsewhere that SDO production in electric discharge may be more effective if at the moment of the discharge ignition there are some SDO molecules in the gas mixture. From this point of view, the gas excitation by a train of subsequent pulses could have led to higher SDO yield.

In our conditions at pure oxygen gas flow rate 15 m/s (the time needed for the gas to flow through the discharge zone is ~ 2 ms), the influence of modulation frequency (applied to CW RF power supply) upon SDO production was studied at constant average RF power loaded into the discharge. Time traces obtained in these experiments are presented in **Fig.45**. The time trace corresponded to SDO luminescence intensity observed with CW RF discharge excitation is presented in **Fig.45a** as a reference. It should be emphasized that for **Fig.45a** CW RF power was 180 W and for **Figs.45b-e** pulsed RF power was 900 W (at the same average RF power of 180 W). Decreasing the RF power modulation frequency from 10 kHz down to 1 kHz (**Figs.45e-b**) resulted in the increase of SDO concentration of about 50%. A transition from modulation frequency of 1 kHz to CW mode with the same average RF power gave the additional growth of SDO concentration of about 25-30%. One can make a conclusion from these experiments that at the same average RF power loaded into the discharge, SDO production is more effective at CW mode of gas excitation.

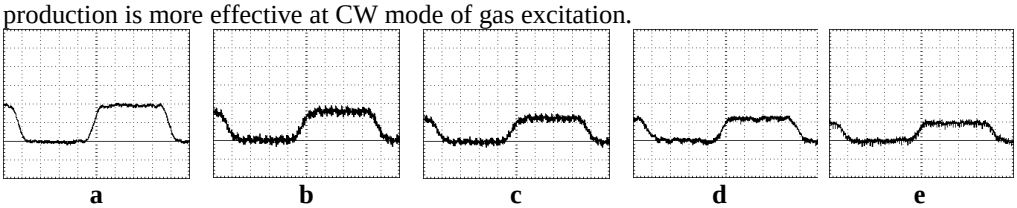

a **b** **c** **d** **e**

Fig.45. SDO luminescence intensity. Pure O_2. P=15 Torr, $V=V_{max}/2$. Average RF power 180 W, RF power supply modulation frequency 1 kHz (b), 5 kHz (c), 7 kHz (d), 10 kHz (e), and CW mode without modulation (a). Relative pulse duration - 20%. Time scale 2.5 ms/div.

Theoretical (CW mode).

The model of the SDO generator with RF slab discharge developed by us earlier was implemented for analyzing how the discharge power, gas mixture pressure and flow rate influence on SDO yield. Presented here results of numerical simulations relate to CW RF discharge with frequency of the exciting wave field 60 MHz at electric generator power in the range 50-800 W. Calculations were made for pure oxygen flow at pressures 7.5, 15, and 30 Torr with linear flow velocity in the discharge zone 15 and 30 m/s. The discharge occupies rectangular volume with inter-electrode gap length 3 mm, transverse size 3 cm, and length along flow 30 cm. Thus, the discharge volume is equal to 27 cm^3. After gas portion leaves the discharge zone plasma decays and excited species and radicals relax. Calculations were made up to 3 and 6 ms, when gas portion approaches location 9 cm down flow at flow velocity 30 and 15 m/s, respectively.

Figs. 46-51 show calculation results for gas flow velocity 30 m/s. **Fig. 46** demonstrates the SDO concentration as a function of discharge power for three values of oxygen pressure at moments 1.67 and 2.83 ms measured from the discharge beginning.

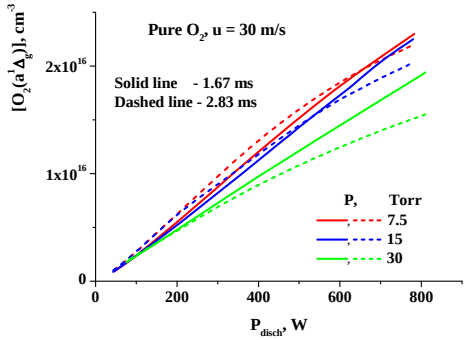

Fig.46. SDO concentration as a function of discharge power for three values of oxygen pressure at moments 1.67 and 2.83 ms from the discharge beginning.

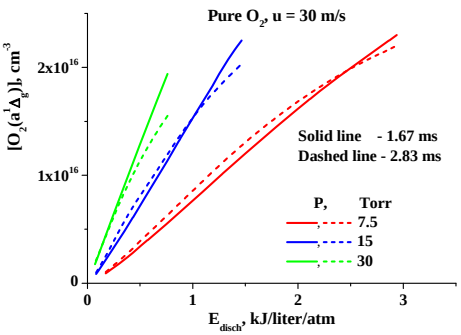

Fig.47. SDO concentration as a function of the specific input energy for three values of oxygen pressure at moments 1.67 and 2.83 ms from the discharge beginning.

SDO concentration is shown in **Fig. 47** as a function of the specific input energy for three values of oxygen pressure at moments 1.67 and 2.83 ms from the discharge beginning. Curve crossings for moments 1.67 and 2.83 ms at pressures 7.5 and 15 Torr is explained by the fact that the SDO concentration continues to grow in after-glow region due to relaxation of O_2 molecules from higher electronic states to $a^1\Delta_g$. At discharge powers lower than some fixed value the SDO concentration approaches maximum in between 1.67 and 2.83 ms. While increasing gas pressure up to 30 Torr the maximum in the SDO concentration moves up-flow to the discharge zone, and curves relating to observation times 1.67 and 2.83 ms do not cross.

It is worth to note that in the model used the near-electrode layers formed in capacitive RF discharge were ignored. The discharge energy release in these near-electrode layers goes mainly to gas heating, thus diminishing the SDO production rate. It was shown in papers (*Starostin S.A., 2002; Ionin A.A., 2005; Proshina O.V., 2006*) that the layer thickness increased for diminished gas pressures. Such effect can lead to reduction of the SDO concentration with gas pressure diminishing. For proper account of this effect it is necessary to develop one-dimensional model of the RF discharge.

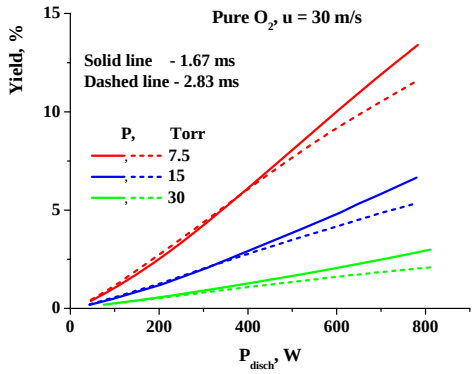

Fig.48. The SDO yield as a function of discharge power at moments 1.67 and 2.83 ms from the discharge beginning for gas pressures 7.5, 15 and 30 Torr.

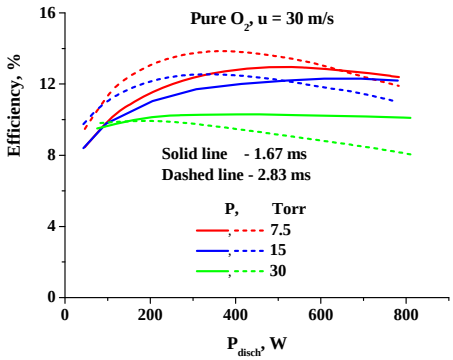

Fig.49. SDO production efficiency as a function of discharge power at moments 1.67 and 2.83 ms from the discharge beginning for gas pressures 7.5, 15 and 30 Torr.

Figs.48 and **49** show calculated SDO yield ($\text{Yield} = \frac{[O_2(a^1\Delta_g)]}{[O_2]+[O_2(a^1\Delta_g)]}$) and its production efficiency as a function of discharge power. The SDO yield is higher at lower oxygen pressure. The SDO production efficiency changes insignificantly with variations of RF discharge power and gas pressure. This is explained by a low sensitivity of the effective reduced electric field value to changes of RF discharge power and gas pressure.

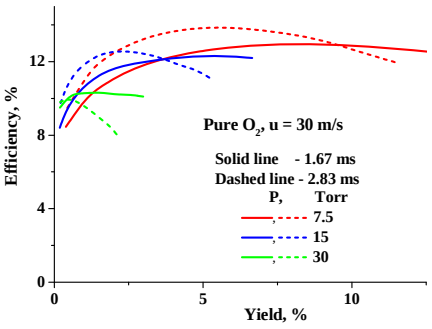

Fig.50. SDO production efficiency as a function of the yield at moments 1.67 and 2.83 ms from the discharge beginning for gas pressures 7.5, 15 and 30 Torr.

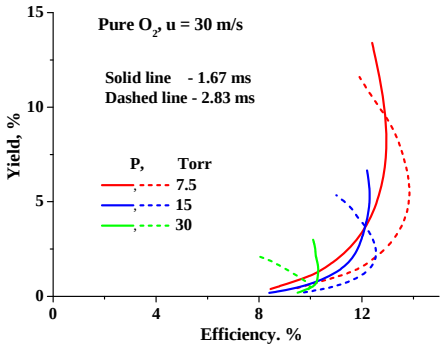

Fig.51. SDO yield as a function of production efficiency at moments 1.67 and 2.83 ms from the discharge beginning for gas pressures 7.5, 15 and 30 Torr.

The electric discharge SDO generators are characterized by two important parameters: the SDO yield and its production efficiency. Correlation between these two parameters is illustrated in **Figs.50** and **51**. Under conditions considered the predicted SDO yield can be as high as 8% at efficiency 12% for gas pressure 15 Torr.

Figs.52-57 demonstrate simulation results for the flow velocity 15 m/s twice diminished in comparison with analyzed above. It is seen that at lower flow velocity the SDO concentration at the generator output saturates as a function of the RF discharge power.

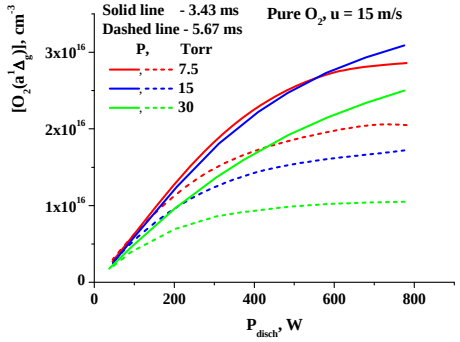

Fig.52. SDO concentration as a function of discharge power for three values of oxygen pressure (7.5, 15, and 30 Torr) at moments 3.43 and 5.67 ms from the discharge beginning.

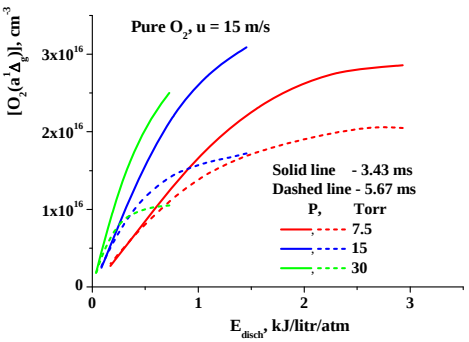

Fig.53. SDO concentration as a function of the reduced energy input for three values of oxygen pressure (7.5, 15, and 30 Torr) at moments 3.43 and 5.67 ms from the discharge beginning.

This effect is explained by two times lengthening of gas portion residence time in the discharge zone and doubled specific input energy, respectively. At gas pressure 15 Torr the SDO yield approaches 10 % with production efficiency 8%.

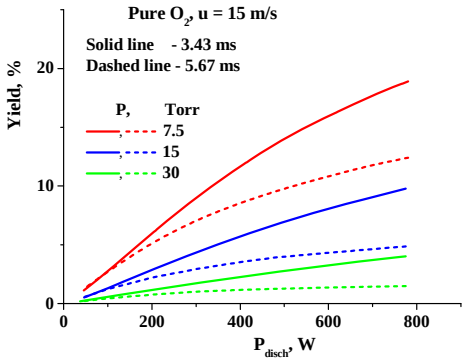

Fig.54. SDO yield as a function of discharge power for three values of oxygen pressure (7.5, 15, and 30 Torr) at moments 3.43 and 5.67 ms from the discharge beginning.

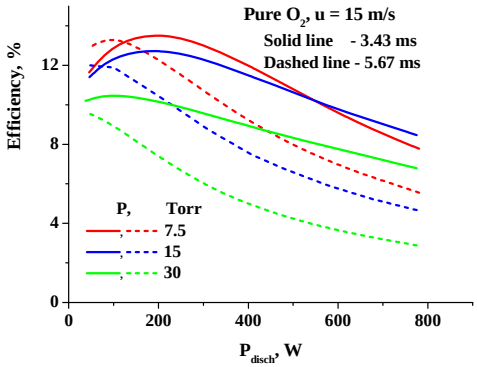

Fig.55. SDO production efficiency as a function of discharge power for three values of oxygen pressure (7.5, 15, and 30 Torr) at moments 3.43 and 5.67 ms from the discharge beginning.

The SDO production efficiency is diminishing with growth of the yield. Reduction of the efficiency and yield is more pronounced at larger distances from the discharge zone (**Fig. 56**). This is caused by SDO relaxation on atomic oxygen in three-body collisions *(Rakhimova T.V., 2005)*. The negative effect of SDO relaxation can be improved to a large degree by virtue of addition of small concentrations of NO or NO_2, which effectively remove atomic oxygen from the mixture *(Ionin A.A., 2009a)*.

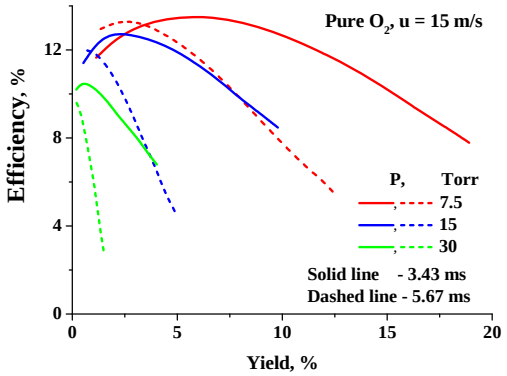

Fig.56. SDO production efficiency as a function of SDO yield for three values of oxygen pressure (7.5, 15, and 30 Torr) at moments 3.43 and 5.67 ms from the discharge beginning.

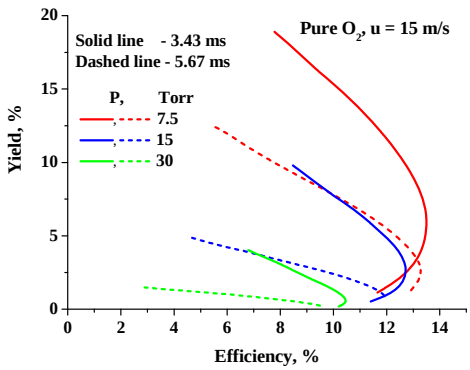

Fig.57. SDO yield as a function of SDO production efficiency for three values of oxygen pressure (7.5, 15, and 30 Torr) at moments 3.43 and 5.67 ms from the discharge beginning.

The SDO production efficiency is diminishing also at the RF discharge power decreasing in the range (200 – 300) W (**Fig. 49** and **Fig. 55**). This is explained by growth of the reduced electric field with diminishing the RF discharge power. **Fig.58** demonstrates E/N variation in time. Though the E/N magnitude falls down with time it remains essentially higher than the value corresponding to the maximum of the $O_2(a^1\Delta_g)$ production efficiency, which is about 12 Td *(Ionin A.A., 2007b)*. The discharge breakdown proceeds for short times about 1 μs. The value of E/N at this phase of the discharge is controlled by nearly equal ionization and dissociative electron attachment to O_2 rates (moment 1 in **Fig.58** and column 1 in Table 1). Further, concentration of the negative ions grows, and their destruction in collisions with O atoms and electronic excited O_2 molecules leads to growth of electron number density. The electron concentration balance on this phase is controlled by processes of electron attachment and detachment (moments 2 and 3 in **Fig.58**; second and third columns in Table 1).

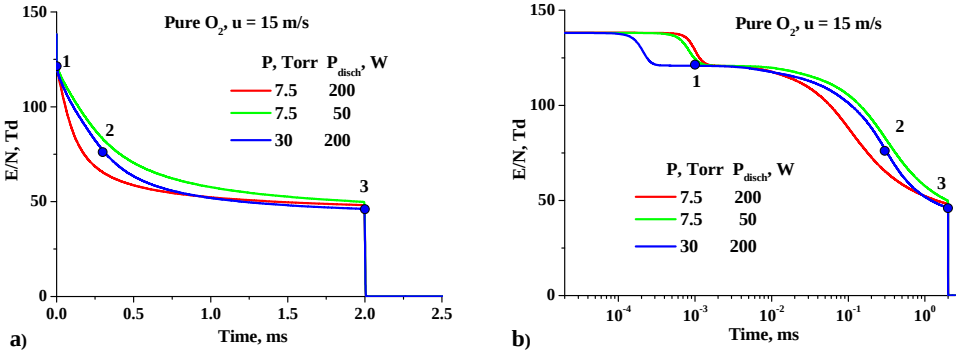

Fig.58. The reduced electric field strength as a function of time: (a) linear time scale; (b) logarithmic time scale. Full circles relate to moments indicated in Table 1.

At lower gas pressures while keeping constant the discharge power the energy input per O_2 molecule increases resulting in increasing detachment processes role at shorter times (compare blue and red curves in **Fig.58**).

Table 1. Shares of various processes in production and decay of free electrons at the moments 1 μs (1), 300 μs (2), and 2 ms (3) measured from the discharge beginning. P = 30 Torr, P_{disch} = 200 W, u = 15 m/s.

#	Time moments	1 μs	300 μs	2 ms
	Reaction			
1	$O_2 + e \rightarrow O^- + O$	-100%	-100%	-100%
2	$O_2(a^1\Delta_g) + e \rightarrow O^- + O$			-6%
3	$O_2(b^1\Sigma_g^+) + e \rightarrow O^- + O$			-9.1%
4	$O_2 + e \rightarrow O_2^+ + e + e$	+99%	+9.3%	
5	$O^- + O \rightarrow O_2 + e$		+21%	+30%
6	$O^- + O_2(a^1\Delta_g) \rightarrow O + O_2 + e$		+10%	+41%
7	$O^- + O_2(b^1\Sigma_g^+) \rightarrow O + O_2 + e$		+43%	+43%
8	$O_2^- + O \rightarrow O_3 + e$		+8.5%	
9	$O_2^- + O_2(b^1\Sigma_g^+) \rightarrow O_3 + e$		+5.6%	

It is of practical interest to study RF pulse-periodic discharges in oxygen for SDO production. The gas portion while transporting through the discharge zone undergoes repeatable action of the discharge. The number of pulses affecting on this portion varies with the pulse repetition rate while the average power depends on peak power and relative pulse duration. We have performed numerical simulations for: oxygen pressure 15 Torr; gas flow velocity 30 m/s; relative pulse duration 20%; repetition rates 1, 2, 4, 6, 8, and 10 kHz; and peak RF discharge power 1100 W. The average RF discharge power amounts 220 W.

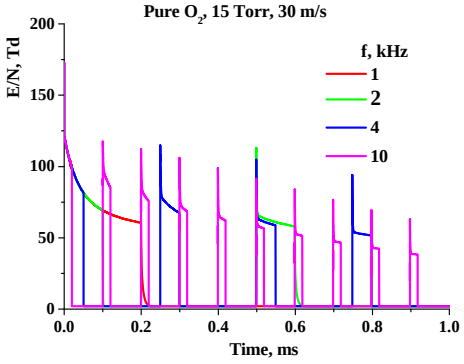

Fig.59. Time history of the reduced electric field strength for various repetition rates of RF pulses. Relative pulse duration for RF field pulses is 20%.

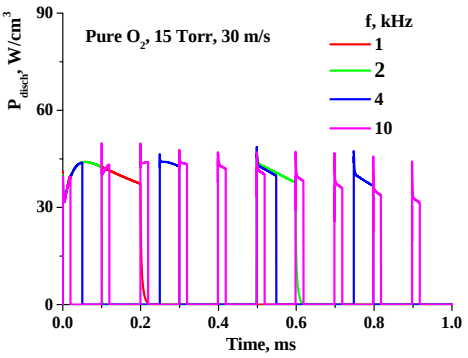

Fig.60. Time history of the RF discharge power for various repetition rates of RF pulses. Relative pulse duration for RF field pulses is 20%.

Fig.59 shows time evolution of the reduced electric field strength for repetition rates: 1, 2, 4, and 10 kHz. In the course of time E/N parameter magnitude falls down from pulse to pulse. As it was said above, this is explained by accumulation of negative ions and electron detachment processes in collision processes of negative ions with O atoms and $O_2(a^1\Delta_g)$ or $O_2(b^1\Sigma^+_g)$ molecules. **Fig.60** shows how the discharge power changes from pulse to pulse for the same conditions as in **Fig.59.**

Let us note that in the experiments the discharge power was controlled. In the theoretical model the supply voltage and ballast resistor serve as the fit parameters to achieve the same discharge power as one realized experimentally. The voltage value and ballast resistor found in this way provide the discharge average power constant within repetition frequency range (1–10) kHz at variance less than 5%.

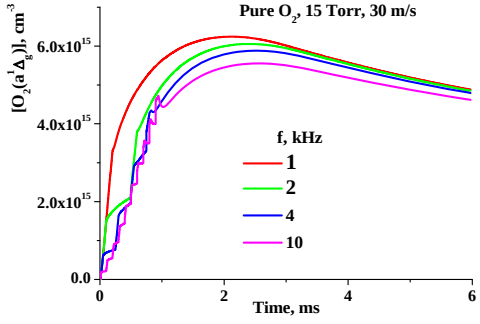

Fig.61. Time dependence of SDO concentration for various repetition frequencies of RF pulses. Relative pulse duration for RF field pulses is 20%.

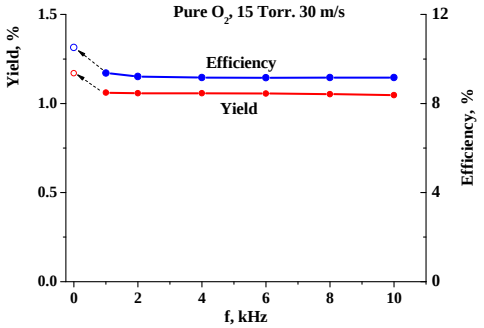

Fig.62. Concentration of $O_2(a^1\Delta_g)$ and its production efficiency as functions of RF pulse repetition frequency at the time moment 6 ms. Relative pulse duration for RF field pulses is 20%.

Fig.61 shows evolution in time (along the flow) the SDO concentration for various RF discharge pulse repetition rates. **Fig.62** demonstrates the SDO yield and its production efficiency in dependence on repetition rate of the RF discharge pulses. The SDO yield and its production efficiency practically do not depend on pulse repetition rate of the RF discharge. They both are slightly lower than values predicted for CW mode of RF discharge operation at the power equal to the average power of pulse-periodic regime. The last are shown in **Fig.62** by open circles. This result does not coincide with above experimental data. Further studies are needed.

Conclusions.

SDO production depending on gas mixture content, gas flow velocity, low-frequency modulation of RF power and RF discharge power was experimentally studied. The oxygen pressure increase resulted in significantly SDO concentration growth at the same specific input energy. SDO yield increased with gas pressure decreasing at the same RF discharge power. In the experiments the highest SDO yield was obtained at gas pressure of 7.5 Torr. Two fold gas flow deceleration (down to 15 m/s) about doubled SDO concentration rise at gas pressure 7.5 Torr and resulted in 10-15% rise at 30 Torr. At both gas flow velocities (30 m/s and 15 m/s) the maximal SDO yield was observed at gas pressure of 7.5 Torr .

The SDO yield saturation was observed with specific input energy rising at different gas pressures. SDO production in helium content gas mixture was also studied. Helium dilution of oxygen resulted in SDO concentration and yield increase considerably (as much as about twice). The study of influence of RF power modulation frequency on SDO production was carried out with averaged input power being constant. The frequency modulation decrease from 10 to 1 kHz resulted in SDO concentration rise by about 50%. In CW RF discharge mode SDO concentration increased on 25-30% at the same averaged input power. Thus, at the same averaged input power of RF discharge, the CW RF discharge is the most efficient for SDO production.

The model developed was further modified to do simulations of CW and pulse periodic RF discharges. A reasonable agreement between experimental and theoretical data on SDO production in CW and pulse-periodic RF discharges in oxygen is observed.

The SDO yield and its production efficiency practically do not depend on pulse repetition rate of the RF discharge. They both are slightly lower than values predicted for CW mode of RF discharge operation at the power equal to the average power of pulse-periodic regime. This result does not coincide with above experimental data. Further studies are needed.

2.2. Possibility study of a technique of compulsory atomic iodine production.

Introduction.

The success obtained up to now in the development of electrically driven singlet oxygen generators makes it possible to produce singlet oxygen with a yield $Y = [O_2(^1\Delta_g)] / [O_2(^1\Delta_g)] + [O_2(^3\Sigma_g)]$, where $[O_2(^1\Delta_g)]$ and $[O_2(^3\Sigma_g)]$ are the concentration of oxygen in excited and the ground states, respectively, over the threshold level (Y = 15% at the room temperature). But active medium small signal gain obtained up to now are too low. Thus, applications of low losses and highly reflecting mirrors are necessary to get CW lasing threshold. Small signal gain (SSG) *G* in the active medium of oxygen-iodine laser can be written as

$$G = \sigma \cdot I_{total} \cdot \frac{(2K_{eq}+1)\cdot(Y-\frac{1}{2K_{eq}+1})}{2[(K_{eq}-1)Y+1]} \quad ,$$

where σ is an amplification cross-section, I_{total} is a total concentration of iodine atoms and $K_{eq} = 0{,}75\exp(400/T)$ is an equilibrium constant. Thus, the SSG value is a function of singlet oxygen yield, iodine atoms concentration and K_{eq} being, in its turn, the temperature dependent parameter. The concentration of iodine atoms can be varied in a wide range using the method of volume instantaneous generation of iodine atoms. The main point of this method is the mixing of singlet oxygen with iodide (CH_3I, CF_3I, etc) followed by fast decomposition of iodide resulting in production of free iodine atoms. Application of the method of volume generation of iodine atoms, as well, could result in the laser pulsed mode, which could provides the high pulse power at low average power. Such a feature could be useful to extend the field of laser application.

Experimental.

The design of experimental set up allowed us to work with chemical SDO generator (SOG) as well as with electric one. Such an opportunity made it possible to evaluate the specific character of electrical SOG and find the ways to fight against negative factors. The schematic diagram of experimental setup is shown in **Fig.63**. The flow from dry chemical SOG consisted of pure nitrogen. Effluent of SOG filled with working solution contained oxygen including excited fraction, nitrogen and water vapor, which pressure was governed by solution temperature and low temperature trap located downstream of SOG. The temperature of trap walls was controlled by alcohol cooled down to -70… - 60^{O}C by liquid nitrogen.

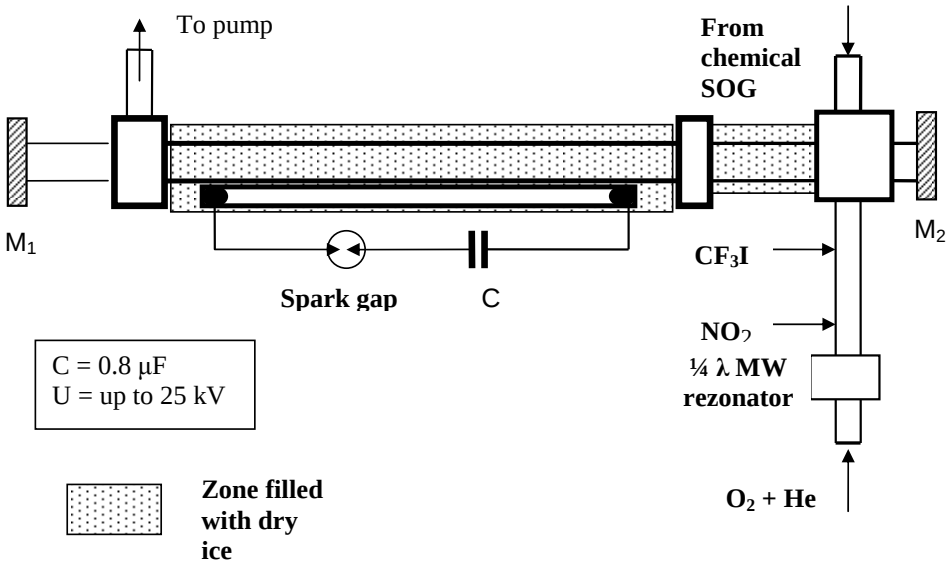

Fig.63. Schematic diagram of experimental setup

The mixture of He with additional oxygen was directed to the laser chamber through a 12mm silica tube passing through a quarter wave MW cavity fed by 150 W output power generator. The tube wall downstream of cavity was coated with HgO layer to scavenge oxygen atoms. Silver coating was also used, but HgO appeared to be more effective.

To monitor oxygen atoms concentration, the injection of nitrogen dioxide eliminating oxygen atoms in the process $NO_2 + O = NO + O_2$ (*Kaufman F., 1961*) can be used. Formation of nitrogen oxide NO in this reaction resulted in appearance of white emission due to photo recombination reaction $NO + O \rightarrow NO_2 + h\nu$. The intensity of this emission is proportional to product of oxygen atom concentration by that of NO. When concentration of injected nitrogen dioxide is enough for total elimination of oxygen atoms the emission disappears. Thus, monitoring of this emission can be used as a source of information on oxygen atoms.

The injector of CF_3I was located downstream of that of NO_2. Such an order of injectors is dictated by necessity of injection of iodide into the mixture free of oxygen atoms.

The mixture of necessary composition comes through the laser chamber made of 24 O.D. silica tube. In the laser chamber the mixture is exposed by UV emission of a flash lamp fed by C = 0.8 μF capacitor charged to 25 kV. The assembly lamp-laser chamber was wound with Al foil to increase the efficiency of UV emission utilization.

The field of initiation and the section located upstream of the lamp are placed into the thermo-insulating vessel filled with “dry ice” to cool the gas flow. The length of the cooled section is 50 cm, 20 cm of which was located upstream of the flash lamp.

The gas handling system made it possible to prepare the mixtures of necessary compositions and to control their flow. The rotameters of different types and pressure gauge VDG-1 and “Metran” were used to control the gas flow rate. To provide the stable gas flow the mixtures were fed from soft polyethylene bags under atmospheric pressure.

The stable cavity of the photo dissociation pulsed iodine laser (PIL) was formed by two spherical mirrors one of which was totally reflecting but transmittance of other was chosen in dependence of task to be solved.

Two thermocouples measuring the temperature of gas flow at the center of laser tube and close to the wall showed that the applied cooling was not enough. The additional cooled 20 cm

section was mounted upstream of the lamp to reduce the active medium temperature. For more correct deriving of the effective temperature of active medium under cooling it was proposed to use the dependence of the PIL performance (output energy, shape of pulse) on iodide density. In the case of subsonic flow the active medium has an increased density in a cold section. Density is inversely proportional to active medium temperature. Thus, assuming the processes governing the PIL performance does not depend on temperature, one can find the temperature by recording the output PIL energy at room temperature and under cooling.

Thus, experiment was held as follows: laser pulses obtained with the different pressures of a mixture He + CF_3I at the room temperature and under cooling were recorded with a digital oscilloscope and pulse energy was derived using previously made absolute detector calibration. **Fig.64** demonstrates the pressure dependence of PIL output at room temperature and under "dry ice" cooling.

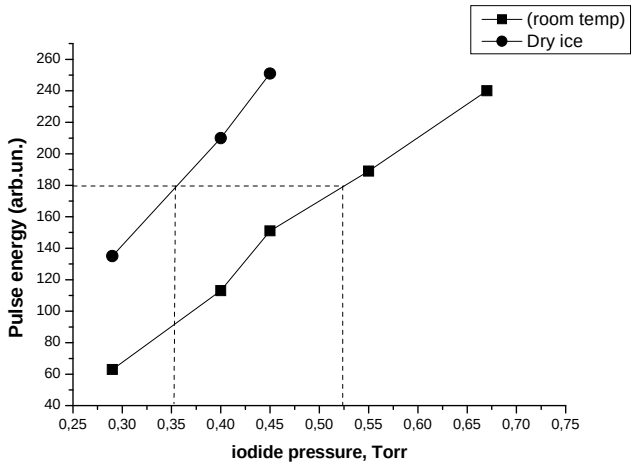

Fig.64. Pressure dependence of PIL output at the room temperature and under "dry ice" cooling.

The temperature of a cooled active medium is derived from the expression $T_{cooled}= 300\cdot(P_{cooled} / P_{room})$, where P_{cooled} and P_{room} are the pressures corresponding to the same output energy at cooling and the room temperature respectively. The temperature values 193K, 210K и 200K were obtained for three pressure values. Thus, one can consider that the temperature of gas flow averaged over the cooled section under our experimental conditions (mixture pressure – 1.5-2 Torr, pump capacity – 22-24 l/s) was 200 ±10K. Thus, the additional section of cooling made it possible to improve active medium cooling.

Active medium kinetics.

Application of electric SOG unlike chemical one results in a certain problem that, being not solved, makes application of such an approach of having no prospects. First of all, it is a result of presence of oxygen atoms in effluents of electric discharge. It is known, oxygen atoms fast react with iodide CF_3I, CH_3I (*Gilles M.K., 1996*). In the case of CH_3I this reaction produces a lot of different compounds, but compound IO is a main product for the case of CF_3I.

$$CF_3I + O = CF_3 + IO \qquad (11)$$

The rate constant for the process (11) is rather high $K_1 = 5{,}8\cdot10^{-12}$ cm^3 s^{-1} (*Atkinson D.B., 1999*), although it yields to that for I_2 ($K = 1{,}4\cdot10^{-10}$ cm^3 s^{-1} (*Payne W.A., 1998*)). In their turn, IO molecules react with oxygen atoms producing free iodine atoms

$O + IO = O_2 + I \quad K_2 = 1{,}5 \cdot 10^{-10}$ cm^3 s^{-1} (12)

In spite the fact that iodine atoms are the source of mixture instability they are not the main reason of energy store relaxation. The influence of radicals CF_3O_2 is more essential. This radical is formed in a three body reaction (13) having rate constant $K_3 = 1,\ 9 \cdot 10^{-29}$ cm^6 s^{-1} (*Caralp F., 1986*)

$CF_3 + O_2 + M = CF_3O_2 + M$ (13)

For radical CH_3 the rate constant of a similar process is $K_3 = 1{,}0 \cdot 10^{-30}$ cm^6 s^{-1} (*Keiffer M., 1987*). As it was shown (*Vagin N.P., 1991*), radical CF_3O_2 is a strong quencher of both singlet oxygen and excited iodine atoms in processes

$O_2(^1\Delta_g) + CF_3O_2 = O_2(^3\Sigma_g) + CF_3O_2$, $K_4 = 4.5\text{x}10^{-11}$ cm^3 s^{-1} (14)

$I(^2P_{1/2}) + CF_3O_2 = I(^2P_{3/2}) + CF_3O_2$ $K_5 = 2.5\text{x}10^{-11}$ cm^3 s^{-1}. (15)

Thus, the influence of processes (14, 15) can result in losses of singlet oxygen yield in a stage of active medium forming, i.e. filling of a laser chamber.

The numerical model taking into account the processes governing the singlet oxygen behavior was developed to estimate the importance of this effect.

$CF_3I + O = IO + CF_3$	$K = 5.8\text{x}10^{-12}$
$O + IO = O_2(X) + I$	$K = 1.5\text{x}10^{-10}$
$CF_3 + O_2(X) = CF_3O_2$	$K = 8\text{x}10^{-13}$
$IO + IO = O_2(X) + 2I$	$K = 8.2\text{x}10^{-11}$
$O_2(a) + I = O_2(X) + I^*$	$K = 7.8\text{x}10^{-11}$
$O_2(X) + I^* = O_2(a) + I$	$K = K_5/0.75\exp(401/T)$
$O_2(a) + CF_3O_2 = O_2(X) + RO_2$	$K = 4.5\text{x}10^{-11}$
$O_2(a) + O = O_2(X) + O$	$K = 1.65\text{x}10^{-16}$
$I^* + O = I + O$	$K = 1\text{x}10^{-12}$

Application of the model to analyze the behavior of SDO concentration in the mixture $[O_2] = 1.5*10^{16}$, $[CF_3I] = 1.5*10^{16}$, $[O] = 3*10^{14}$ cm^{-3}, Y = 0.2, corresponding to experimental conditions of (*Vagin N.P., 1991*), shows the SDO concentration drops to the zero for $5*10^{-4}$ s (**Fig.65**).

Under volume pump capacity 20 l/s, the linear flow velocity in a laser chamber of 22 mm diameter is 52.6 m/s. Thus, practically total loss of SDO occurs at the distance 2 cm. Variation of initial concentration of atomic oxygen shows that two orders of magnitude reduction of oxygen atoms concentration is necessary i.e. down to $[O] = 1*10^{12}$ cm^{-3}. Under this condition, the SDO concentration drops from $[O_2(^1\Delta_g)] = 3*10^{15}$ cm^{-3} to $[O_2(^1\Delta_g)] = 1{,}9*10^{15}$ cm^{-3} for time of laser chamber filling 0.01s. The value of yield drops from 20 to 12,6 % (**Fig.66**), that is to the value that still exceeds the threshold corresponding to the temperature of dry ice used for active medium cooling (T = 195K, Y = 8%).

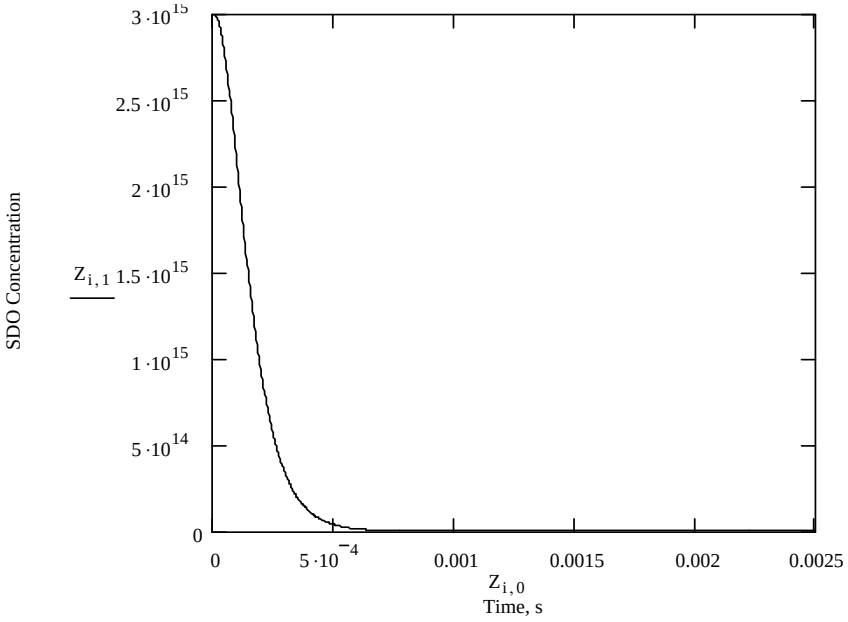

Fig.65. Time dependence of SDO concentration at [O] = $3*10^{14}$ cm^{-3}

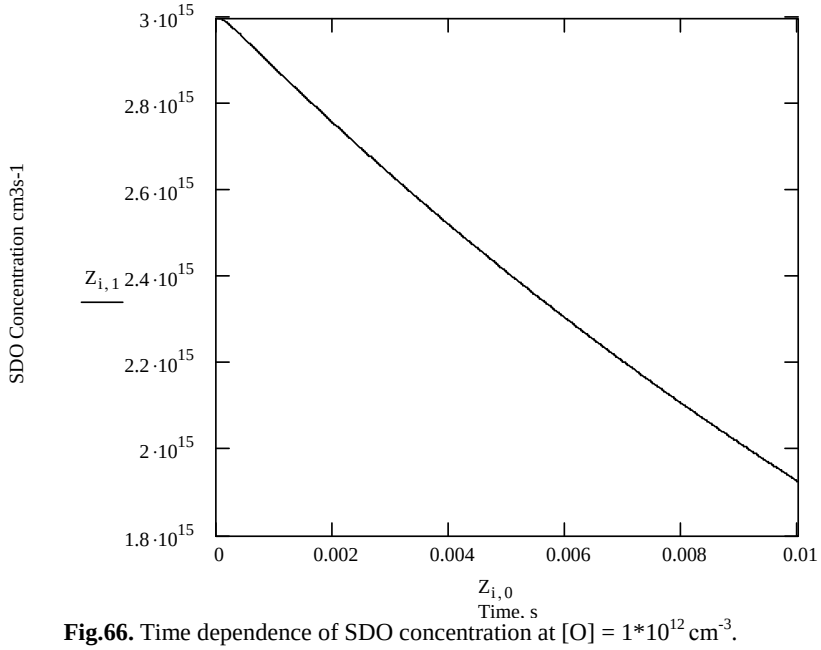

Fig.66. Time dependence of SDO concentration at [O] = $1*10^{12}$ cm^{-3}.

Thus, solving the problem of elimination of oxygen atoms from the SDO flow becomes the necessary condition to realize pulsed mode of oxygen - iodine laser with electric SDO generator. Both, heterogeneous ($HgO + O = Hg + O_2$) as well as homogeneous ($NO_2 + O = NO + O_2$) processes can be used for this purpose. But achievement of necessary value [O] =

$1*10^{12}$ cm $^{-3}$ is not obvious and needs experimental conformation. Thus, experimental modeling of active medium by addition of effluents from electric SOG to the flow from a standard chemical SOG is proposed.

It is known that SDO is a very stable molecule and it has low efficiency of quenching in collisions with molecules of inherent to COIL. Therefore, chemically produced SDO can be easily transported to the place of utilization. Another situation takes place in the case of electrically produced SDO. One can suppose that the species produced in the process of SDO generation in plasma are the effective SDO quenchers. One of species generated in the oxygen plasma is atomic oxygen. To measure the concentration of atomic oxygen produced in electric discharge one can use the method of titration with nitrogen dioxide NO_2 (*Kaufman F., 1961*). Being added to the mixture containing oxygen atoms, NO_2 scavenges them in reaction $NO_2 + O = NO + O_2$.

At this time the white emission due to recombination $NO + O = NO_2 + h\nu$ increases and then drops and disappears when amount of NO_2 is equal to O atoms concentration. This method was used to study the dependence of oxygen dissociation on experimental conditions to select a most acceptable mode. **Fig.67** demonstrates dependence of concentration in investigation section of oxygen atoms generated in the MW cavity on pressure of O_2 : He = 1 : 2 mixture for different levels of MW power. As one could expect, the oxygen atoms concentration [O] increases with MW power. But the increase of [O] with pressure does not seem obvious. The dissociation efficiency, i.e. the ratio of oxygen atoms concentration to that of molecular oxygen, within the variation of experimental parameters increases too. One should pay attention that the dissociation efficiency is more sensitive to MW power at increased pressure of oxygen mixture (**Fig.68**).

The similar dependences have place for pure oxygen but in this case the dissociation efficiency is about a half of that for oxygen – helium mixture.

It is well known that the atomic oxygen reacts with molecular iodine producing iodine atoms in the chain of reactions $O + I_2 = IO + I$ and $IO + O = I + O_2$.

This mechanism is used as an iodine atoms source in the electrically driven oxygen iodine laser. Similar reactions take place for CH_3I (*Gilles M.K., 1996*): $CH_3I + O = IO + CH_3$ and $IO + O = I + O_2$.

But unlike NO_2 each molecule of CH_3I scavenges two oxygen atoms. One can suppose that this reaction can be used to measure oxygen atoms concentration too. To check this idea the mixture CH_3I : He = 1 : 329 was admixed to the effluent of MW generator up to the concentration resulting in elimination of white emission. The emission disappeared when 0.5 Torr of CH_3I : He = 1 : 329 was admixed to the 1 Torr of effluent of MW generator operating at the output power 100W. The total pressure in the investigation section was 1.5 Torr. Processing experimental results one can get: $[O] \sim 1 \cdot 10^{14} cm^{-3}$. Note, NO_2 titration under the same MW power and under total pressure of 2.4 Torr gives the value $[O] = 1.5 \cdot 10^{14}$ cm^{-3}. Keeping in mind that [O] increases with pressure, one can see the satisfactory agreement.

One could expect that other iodides CF_3I and HI can be used for this purpose too. But application of CF_3I results in a value of approximately twice as much under the same experimental condition. This fact conflicts with results of a study of reaction of CF_3I and CH_3I with oxygen atoms (*Gilles M.K.,1996*), where it is shown that at practically equal values of rate constants of scavenging oxygen atoms, the yield of IO as a reaction product in the case of CH_3I is only one half of that for CF_3I.

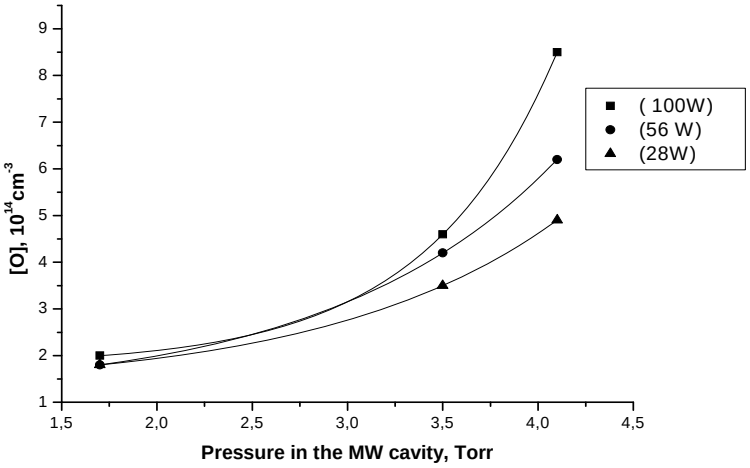

Fig.67. Dependence of [O] on pressure for mixture O_2 : He = 1 : 2

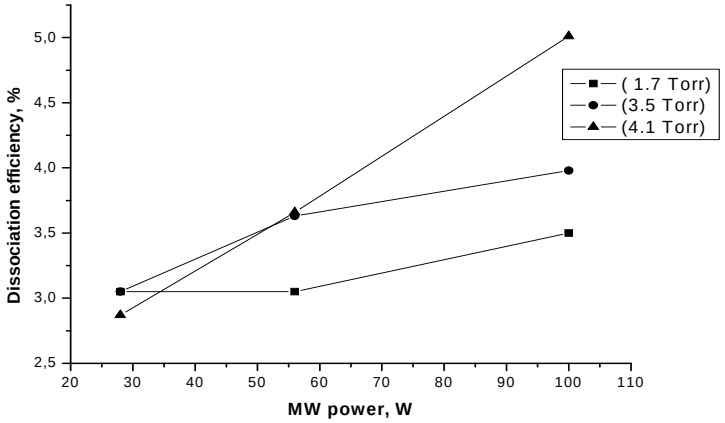

Fig.68. Dependence of dissociation efficiency on MW power for mixture O_2 : He = 1 : 2

Modeling of experiments using chemical SOG.

The object of performed experiments was to model experimentally the active medium of electrically driven oxygen iodine laser. To provide it, the chemical singlet oxygen generator (SOG) was used in common with SOG driven by MW discharge.

In first experiments, the cooled section upstream of initiation lamp was absent and iodide injector was located just upstream of lamp. Iodide injection was produced through the toroidal injector located on the laser axis. Small injector diameter made difficulties for laser alignment. The experiment was held at 1.54 Torr of chemically produced oxygen pressure and 0.6 Torr of iodide partial pressure.

The idea of the experiment was to determine the values of singlet oxygen threshold at room temperature and under cooling. In this case the threshold yield means the yield value

corresponding to appearance of lasing effect in the laser cavity with none zero losses. Such a value of yield corresponds to not only positive gain but to gain exceeding losses. It is clear this value exceeds usually used one defined by expression $Y_{th} = (2K_{eq} + 1)^{-1}$.

Unexcited oxygen was added to the flow of chemically produced oxygen containing the fraction of singlet state up to suppression of lasing. The room temperature experiment is necessary to evaluate the value of singlet oxygen yield Y_0, at the exit of the chemical SOG. This value was found from the expression

$$Y_{th\,300} = \frac{Y_0}{1 + \frac{M_{O\,2\,add}}{M_{Cl\,2}}}$$

where Y_{th300} is the room temperature value of yield, Y_0 is a value of yield at the SOG exit, M_{Cl2}, M_{O2add} are the flow rates of chlorine and additional oxygen respectively. The value Y_{th300} = 0.182 was derived by modeling with obtained previously values of losses and initiation parameters. From here it follows Y_0 = 0,278.

The similar procedure was performed under cooling, but at this case the value of $Y_{th(T)}$ was derived using the known values of Y_0, M_{Cl2}, M_{O2add}. The value obtained $Y_{th(T)}$ = 0.17 corresponded to active medium temperature T = 278K and was in contradiction with temperature measurements. The experimental results are presented in **Fig.69** and **Fig.70**.

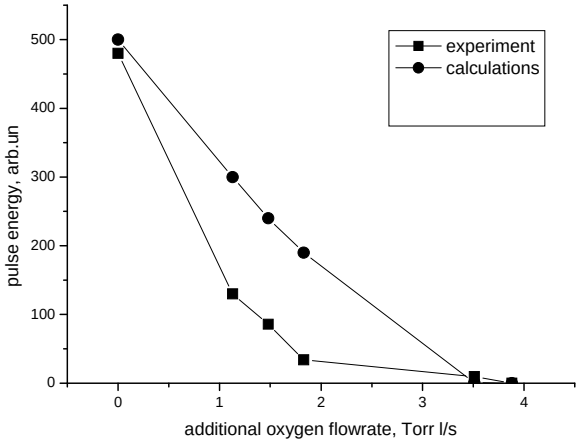

Fig.69. Influence of additional unexcited oxygen on laser output energy at room temperature

For the room temperature the model and experiments with a satisfactory accuracy give the value Y = 0.19 of threshold yield. But another situation takes place under cooling. In this case experimentally obtained value Y = 0.17 seems to be very high.

Indeed, assuming the temperature of active medium is equal to that measured in the experiments with PIL, 200K, one can find the required value of yield by comparison of experiments under cooling and under the room temperature. In real conditions the laser effect occurs when the gain slightly exceeds the level of losses. Assuming the laser resonator parameters are constant, one can state that the lasing suppression happens at the same small signal gain value. For the room temperature Y = 0.19. For T=200K the same small signal gain takes place at Y = 0.095 which is much lower than that obtained in experiment. What can be the reason of such a discrepancy?

We think, taking into account the possible presence of water vapor in active medium, that the decrease of initiation taking place under cooling can be responsible for this effect.

Observed decrease of PIL output energy following the filling of a chemical SOG with working solution is an evidence of water vapor presence. The energy dropped from $1{,}5x10^{-4}$ arb.un being at dry SOG down to $0{,}95\ x10^{-4}$ arb.un. It is possible this fact is a result of low efficiency of low temperature trap. Water vapor having the pressure exceeding saturation one for temperature of laser chamber walls can condense. The saturation pressure is as high as 10^{-3} and 10^{-2} Torr for -74.7^0C and -58.7^0C, respectively. Such a level of water vapor pressure was detected by intracavity spectroscopy method at a similar setup at pump capacity significantly lower that used in our experiment. It is clear the increased pump capacity does not improve the trap efficiency.

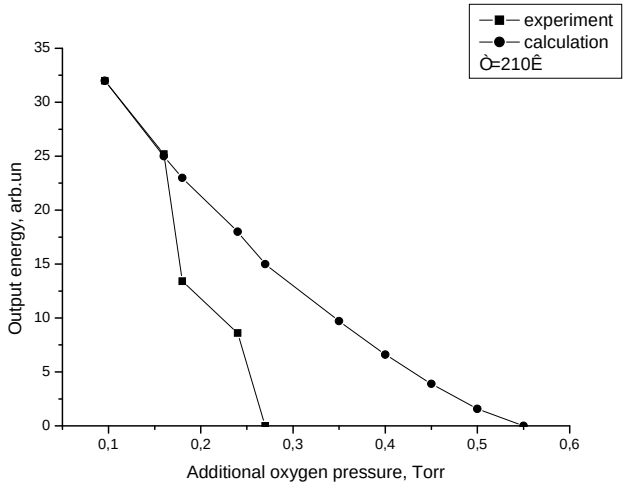

Fig.70. Dependence of output energy on additional oxygen pressure for cooled mixture.

This hypothesis was proved experimentally by observing the degradation of output energy in a process of laser chamber cooling. The initial energy of $1.19\ x10^{-4}$ arb.un dropped down to $0.75x10^{-4}$ arb.un. in 20 minutes after "dry ice" loading. Assuming the temperature of active medium in this moment was 200K and density is half as much, again one could expect output energy of $1.78\ x10^{-4}$ arb.un. Real value was only $0.75x10^{-4}$ arb.un. which corresponds to 2.4 times less of iodine atoms production in photolysis. Thus, one can state that under condition of normal initiation our experimental setup makes it possible to get laser threshold at Y = 0.11 which is obtained at practically all experiments on generation of singlet oxygen in electric discharge. To understand how the products of electric discharge in oxygen influence on laser threshold the comparative experiments were performed with MW discharge being off and on. The results are presented in **Fig.71**.

Being switched on, MW discharge produces singlet oxygen with yield of about Y = 0.1 – 0.15 in a flow of additional oxygen. Let us assume for certainty that Y = 0.1. In this case singlet oxygen yield after mixing increases up to Y = 0.257 for $O_{2\ add}$ = 1.83Torr l/s. As it seen from **Fig.71** laser energy at such a value of yield should be about 100 arb.un. But energy of only E = 62 arb.un. was detected in experiment. At lower MW power the laser energy was 53 arb.un. while it should be two times higher. Thus, one can conclude that the flow from MW discharge contains not only singlet oxygen but any products decreasing gain in the active medium. As it was noted above, atomic oxygen reacting with iodide and forming effective singlet oxygen quencher CF_3O_2 can be this product. Thus, it follows from the experiments that the methods used to eliminate oxygen atoms were not effective enough to reduce oxygen atoms

concentration to the acceptable level. Optimization of the active medium parameters to minimize the bad admixtures to the acceptable level will be the object for future investigations.

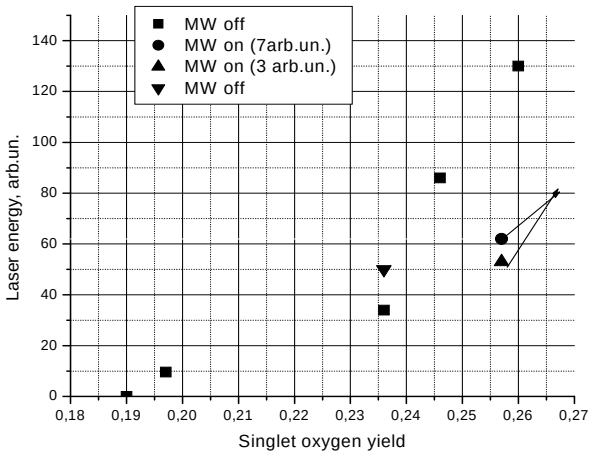

Fig.71. Influence of excitation of additional oxygen flow by MW on laser performance.

Optimization of DOIL working medium.

The results obtained in the experiments on modeling of a DOIL working medium by means of a chemical singlet oxygen generator were the base for experiments on obtaining the lasing threshold for DOIL. In this case the chemical singlet oxygen generator was cut off. The preliminary work on mirrors selection for low loss cavity was performed. The selection was performed by comparison of the iodide pressures corresponding to the threshold of lasing for purely photodissociation initiation of the iodide-helium mixture with lesser oxygen content for each couple of mirrors. Thus, the couple of mirrors with 0,1% transmission which demonstrated the best result was selected.

The experiments were started in about 30 min after filling the facility in with dry ice to achieve the total cooling. The working mixture contained about 0.5 Torr of CF_3I, 0.2 Torr of O_2 and 1.5 Torr of He. The total pressure of oxygen-helium mixture in a MW cavity was as high as 2 Torr. To our regret, the lasing threshold was not detected within all range of experimental parameters.

The experiments on observation of lasing photodissociation pulsed iodine laser operation on the mixture of iodide with oxygen admixtures were performed to evaluate the reasons of our negative result. At that, the oxygen flow before mixing with iodide was passed through MW cavity. Thus, one could change the yield of singlet oxygen in a flow by variation of MW power or its switching on or off. The experiments were performed at the room temperature as well as under cooling by solid carbon dioxide.

Unfortunately, at high iodide pressure the photodissociation laser pulse parameters were practically insensitive to singlet oxygen yield. Otherwise, at operation close to threshold (low iodide concentration) the pulse form was too sensitive to operation conditions, thus, resulting in significant results scattering. Nevertheless, the results processing showed that the laser pulse appeared earlier and it had higher amplitude when MW was on (**Fig.72**).

The results obtained demonstrate that for the time of laser chamber filling singlet oxygen is not quenched totally by CF_3O_2 radicals formed in reaction of iodide with oxygen atoms as it

was predicted by numerical modeling. The possible reasons of this discrepancy can be both inaccuracy in rates constants and presence of processes being not accounted in a model. Our recent experiments on observation of dynamics of iodine atoms concentration in post discharge stage showed the rapid drop of iodine atoms concentration in a mixture containing molecular oxygen.

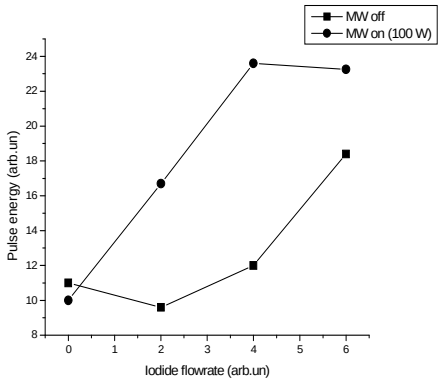

Fig.72a. Influence of MW discharge on PIL performance

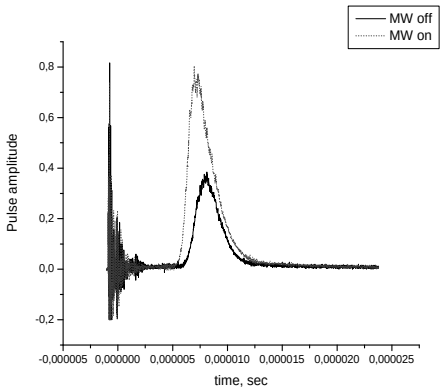

Fig.72b. Influence of MW discharge on PIL pulse shape

Following results of investigation of pulsed photolysis of C_2F_5I – oxygen mixture (*AndreevaT.L., 1997*), one can suppose that the recombination process $RO_2 + I \rightarrow RO_2I$ takes place in our experiments too. This process results in elimination of quencher from laser medium. It follows from investigations performed the more detailed study of active medium kinetics of a pulsed oxygen-iodine laser with forced volume generation of iodine atoms is necessary. Nevertheless, one can state the working mixture formed by mixing iodide with oxygen passing through electric discharge is more stable than one could expect.

Thus, taking into account this circumstance, one can expect that iodide CF_3I could be a promising donor of iodine atoms for DOIL. Having less rate of production of iodine atoms in reactions with oxygen atoms as compared to molecular iodine (reactions 12 and 13) this iodide has a lot of merits in operation (**Table 2**). Among them we can call high saturation pressure (about 6 bar at 300K), low molecular weight being practically one half of that for I_2. The latter can be essential for better mixing and, thus, higher active medium uniformity. Besides, unlike molecular iodine CF_3I is about six orders of magnitude less effective in quenching of excited iodine atoms.

Table 2.

iodide	CF_3I	I_2
Molecular weight	158	254
Saturation pressure	6 bar (300K) 45 Torr (200K)	0.1 Torr (285K) 10^{-4} Torr (226K)
Formation rate constant	$5.8x10^{-12}$	$1{,}4\cdot10^{-10}$
efficiency of I* quenching	$2x10^{-17}$	$(3\text{--}8)x10^{-11}$

Theoretical.

The gas mixture flowing out of an electric discharge singlet oxygen generator is mixed with a stream of iodides serving as donors of iodine atoms. In order to model interaction of these flows chemical reactions between iodides and oxygen atoms and other products of the discharge should be incorporated into the model.

Our theoretical model of pulse discharge in typical gas mixtures used in the experiments was developed on basis of our previous versatile program package allowing for variation of gas composition and properties. It is required an extension of data base for electron scattering cross sections and rate constants for chemical and ion-molecule reactions for new gas components. The program package incorporates self-consistent solving of a system of general kinetic equations (including reactions of excited and non-excited neutral species, radicals, charged particles and so on), of the Boltzmann equation for the electron energy distribution function, of electric circuit equations, of photon number balance in laser cavity and of thermal balance equation.

While developing the model of a pulse discharge in the experimental mixture with He as the buffer gas and CF_3I as the iodine donor, the model previously created for description of an electric discharge singlet oxygen generator (*Vagin N.P., 2006*) was taken as a basis. It was verified by comparison of computed discharge parameters with the experimental values for gas discharge in the mixture flowing out of the chemical singlet oxygen generator (*Vagin N.P., 2003*). The choice of the mixture for modeling purposes is explained by existing data on electron scattering cross sections from CF_3I, a weak influence of He on plasma processes and reliability of data on electrophysical and thermophysical properties of helium. Besides, the experimental data (*Vagin N.P., 1995*) on characteristics of the pulsed chemical oxygen-iodine laser with iodine atoms production in the longitudinal discharge are well reproduced from one run to another.

In the course of discharge model doing, a problem appears to collect published information about electron scattering cross sections and plasma-chemical reactions where initial species, radicals, positive and negative ions produced in the discharge are involved. With respect to CF_3I molecules there exists rather full information, which allows us to minimize uncertainty in values of rate constants. The model (*Vagin N.P., 2006*) was extended by addition new processes taking place in mixtures containing CF_3I. These are: ionization, dissociation, dissociative attachment, dissociative electro-ion and ion-ion recombination, reactions of chemical species formed in the discharge with oxygen, molecular and atomic, and singlet oxygen and excited iodine atoms quenching by produced species. Processes of CF_3I electron-impact dissociation possess the greatest uncertainty. In the energy losses spectrum of scattered electrons two processes can be distinguished with the thresholds 4.7 and 7.2 eV. These processes can be ascribed to dissociation of CF_3I molecules proceeding via compound states. There is no information about paths for decomposition of the excited molecules, and about amplitude of cross sections. The higher-threshold process can result in dissociation into CF_3 and I in the ground or excited state (the upper 1.315-μm laser level). Some argument in favor of appearance of the excited atoms gave Ref. (*Pleasance L.D., 1975*) where the laser action was observed after the pulse discharge in CF_3I+N_2 mixture.

For modeling iodine laser operation the well established data on energy exchange between atomic iodine and singlet delta oxygen as a function of gas temperature and stimulated emission cross section were taken from (*Yuryshev N.N., 1996*).

In the thermal gas energy balance, all known sources of gas heating in plasma were incorporated including relaxation of the singlet oxygen in gas flow from the chemical SOG. Gas-dynamic expansion rate for the experimental conditions (about 140 μs) is comparable with the laser pulse duration. Therefore, the transition from the isochoric mode of expansion to isobaric one was described approximately following (*Vagin N.P., 2006*).

The set of electron scattering cross sections for CF_3I molecules shown in **Fig.73** is a result of our swarm data analysis of (*De Urquijo J., 2007*) based on cross sections from (*Christophorou L.J., 2000*) and from (*Marienfeld S., 2006*). Fitting of cross sections to match the swarm data allows us to achieve rather good agreement with measurements illustrated in **Figs. 74-76**. In particular, measured electron drift velocity in mixtures of CF_3I with nitrogen (*De Urquijo J., 2007*) is compared with results of our simulations with the cross sections shown in **Fig.73** where curves 1-5 are for electron impact dissociation of CF_3I, curves 6-9 are for different ionization channels leading to formation of CF_3I^+, I^+, CF_3^+ and CF_2I^+ ions, respectively.

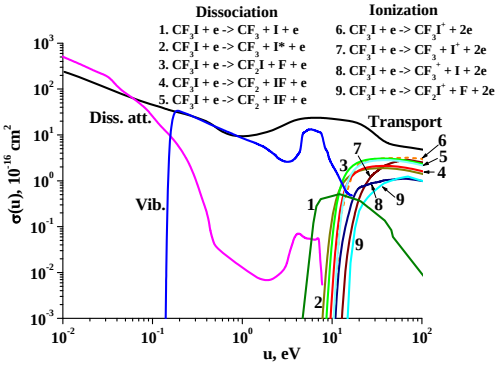

Fig. 73. Cross sections for electrons scattering from CF_3I molecules

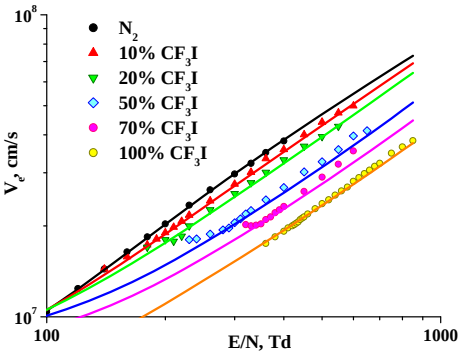

Fig. 74. Swarm analysis for CF_3I – N_2 mixtures, electron drift velocity.

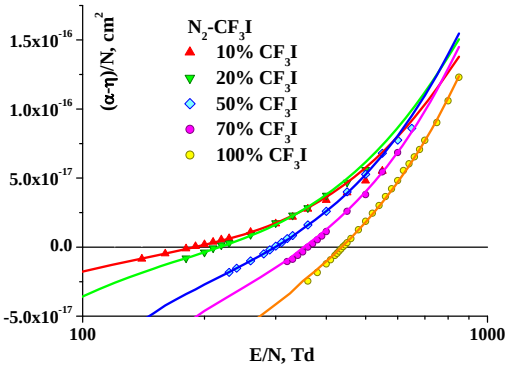

Fig.75. Swarm analysis for CF_3I – N_2 mixtures, effective ionization rate.

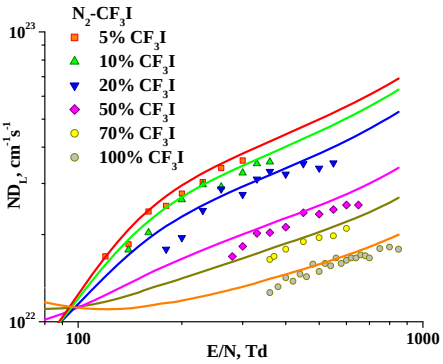

Fig. 76. Swarm analysis for CF_3I – N_2 mixtures, longitudinal diffusion coefficient.

Concluding, our full kinetic model incorporates all essential processes in plasma in a mixture containing oxygen with high percentage of the singlet delta oxygen (SDO), He as a buffer gas and CF_3I as a donor of iodine atoms. Dissociation of oxygen in the discharge leads to accumulation of O atoms up to amount comparable with O_2. It is noteworthy that in the afterglow phase total concentration of excited and ground state iodine atoms slightly grows. This is explained by formation of oxygen atoms in dissociation processes during discharge with followed series of reactions: $CF_3I + O \rightarrow IO + CF_3$, $IO + O \rightarrow O_2 + I$ resulting in iodine atoms formation. Acceleration of singlet oxygen relaxation is associated with laser pulse killing I* with followed energy transfer from singlet oxygen to iodine, relaxation on CF_3O_2 radicals. Besides, the number density of SDO molecules diminishes due to gas dynamic

expansion of gas heated in plasma. The dissociation processes produce about 80% of iodine atoms with near half of which are in the upper laser state. Ion-ion recombination results in production of 10% of atoms, while dissociative ionization is a source of less than 4%. Hence, iodine atoms are produced mainly in dissociation of CF_3I molecules by electron impact. The model developed allows us to perform detailed analysis of processes controlling characteristics of gas laser under study.

Conclusions.

The performed experiments on modeling of the active medium of an electrically driven pulsed oxygen-iodine laser with forced volume generation of iodine atoms showed the parameters of experimental facility make it possible to get laser threshold at 11% of singlet oxygen yield. In spite of the fact that, as it was shown in the previous experiments, the electrically driven source of singlet oxygen provided the required level of singlet oxygen yield, the laser threshold with it was not obtained. It was supposed that process of quenching of the singlet oxygen by CF_3O_2 can be responsible for the negative result. At the same time it was shown that the influence of this process is not so strong. It is supposed that CF_3I can be used as an effective iodine atoms donor for electrically driven oxygen-iodine laser.

The numerical model is developed for description of pulse-periodic oxygen-iodine laser with self-consistent modeling of plasma chemical reactions and electron kinetics. The model developed can be applied for simulations of both self-sustained and non-self-sustained discharges.

3. Conclusions

Experiments on study of influence of nitrogen oxides admixture that decreased atomic oxygen concentration on singlet delta oxygen (SDO) production and quenching were carried out. It was experimentally shown that nitrogen oxide addition resulted in reduction of specific input energy. It was experimentally demonstrated that addition of nitrogen oxide with initial fractions of 0.1 – 0.3% with respect to oxygen concentration resulted in significant enhancement of SDO life-time. The electric discharge chamber was modified: gas flow duct including multi-path cryogenic heat exchanger, dielectric slab channel, and slab electrode system incorporated in the channel for RF discharge ignition. Experiments on SDO production in transverse gas flow slab RF discharge were carried out. SDO production depending on gas mixture content, gas pressure, gas flow rate, low-frequency modulation of RF power and RF discharge power was studied. It was shown that SDO yield increased with gas pressure decrease, gas flow deceleration and helium dilution of oxygen at the same input power. It was demonstrated that CW RF discharge is the most efficient for SDO production at the same averaged input power of RF discharge.

The opportunity of realization of threshold conditions for electrically driven pulsed oxygen-iodine laser with a forced volume generation of iodine atoms was studied both experimentally and theoretically. The experimental facility making it possible to work with electrical and chemical SDO generators in common or separately was developed. The facility developed made it possible to cool working medium with solid carbon dioxide. The measurements performed demonstrated the cooling down to 210K under typical experimental conditions. The experimental modeling of the active medium was performed by using the chemical SDO generator. It has been shown that the facility parameters (cooling depth, used optics quality, etc) makes it possible to get threshold effect at about 11% of SDO yield. The threshold conditions with electric SDO generator only was not achieved. The decrease of initiation level under cooling, which can be a disadvantage of the facility design, can be a possible reason. The numerical model of the laser was developed. The numerical modeling of laser parameters has been performed.

As a result of the work, the theoretical model was formulated for electric discharge SDO generator oxygen-iodine laser with self-consistent description of electron and chemical kinetics taking into account the realistic electric circuit. Along with plasma induced reactions the chemical reactions with iodides and nitrogen oxides were taken into account. The model developed allows for detailed analyzing of processes responsible for laser characteristics. Further, this model was modified to explore pulse-periodic mode of operation of RF discharge with gas flow. The plug flow approximation was adopted where gas mixture components evolution along the flow was considered as time evolution. Numerical simulations demonstrated that the SDO yield and its production efficiency practically do not depend on pulse repetition rate of the RF discharge. They both are slightly lower than values predicted for CW mode of RF discharge operation at the power equal to the average power of pulse-periodic regime.

4. References

Andreeva T.L., et al. // 1997. Quantum Electronics, vol.34, #6, pp.511-516.

Akishev Yu.S., et al. // 1982. Teplofizika Vysokikh Temperatur, vol.20, p.818 (in Russian).

Arakoni R.A., Babaeva N.Y., Kushner M. // 2007. J. Phys. D: Appl. Phys., vol.40. p. 4793.

Atkinson D.B., et al. // 1999. Phys. Chem., vol.A103, pp.6173-6180.

Caralp F., et al. // 1986. Chem. Phys. Lett., vol.129, p.433.

Christophorou L.J., Olthoff J.K. // 2000. J. Phys. Chem. Ref. Data, vol.29, p.553.

De Urquijo J., et al. // 2007. J. Phys. D: Appl. Phys., vol.40**,** p.2205.

Dyatko N.A., et al. // 1985. Fizika plazmy, vol.11, p.730 (in Russian).

Eliasson B., Kogelschatz U. // 1986, Basic Data for Modeling of Electrical Discharges in Gases: Oxygen; Asea Brown Boveri: Baden, Switzerland.

Fujii H., et al. // 2003. "Experimental study of oscillation threshold conditions in a discharge oxygen-iodine laser". 34th AIAA Plasmadynamics and Lasers Conf., 23-26 June 2003, Orlando, Florida, USA; AIAA Paper No AIAA 2003-4028.

Gilles M.K., et al. // 1996. J. Phys. Chem. vol.100, p.14005.

Grigoriev I. S., Meilikhov E. Z. // 1991. Handbook “Physical quantities”, Energoatomizdat, Moscow (in Russian).

Ionin A.A., et al. // 2003. J. Phys. D: Appl. Phys. vol.36. p.982.

Ionin A.A., et al. // 2005. Plasma Physics Reports, vol.31, pp.786–794.

Ionin A.A., et al. // 2006a. "Electric discharge and afterglow kinetics for laser mixtures with carbon monoxide, oxygen and iodine". Final Project Technical Report of ISTC 2415, Moscow, 2006.

Ionin A.A., et al. // 2006b. "Singlet delta oxygen production in self-sustained and non-self-sustained slab discharges". Proc. SPIE, vol.6101, pp.516-530.

Ionin A.A., et al. // 2007a. Proc. SPIE, vol.6346, p.63463I.

Ionin A.A., et al. // 2007b. J. Phys. D: Appl. Phys., vol.40, pp.R25-R61.

Ionin A. A., et al. // 2009a. J. Phys. D: Appl. Phys., vol.42, p.015201.

Kaufman F. // 1961. Prog. React. Kinet. vol.1, p.1.

Keiffer M., et al. // 1987. J. Phys Chem., vol.A91, p.6026.

Marienfeld S., et al. // 2006. J. Phys. B: At. Mol. Opt. Phys., vol.39, p.105.

Payne W.A., et al. // 1998. J. Phys Chem., vol.A102, pp.6247-6250.

Pleasance L.D., Weaver L.A. // 1975. Appl. Phys. Lett., vol.27, p.407.

Proshina O.V., et al. // 2006. J. Phys. D: Appl. Phys., vol.39, pp.5191–5200.

Rakhimova T.V., et al. // 2003. "Radio-frequency plasma generator of singlet oxygen in O_2 and O_2:Ar(He) mixtures". 34th AIAA Plasmadynamics and Lasers Conf., 23-26 June 2003, Orlando, Florida, USA; AIAA Paper No AIAA 2003-4306.

Rakhimova T.V., et al. // 2005. 36th AIAA Plasmadynamics and Lasers Conf. (Toronto, 6–9 June 2005) AIAA Paper 2005-4918.

Starostin S.A., et al. // 2002. Plasma Physics Reports, vol.28, pp.63–70.

Vagin N.P., et al. // 1991. Sov. J. Quant. Electron., vol.18, #1, p.33.

Vagin N.P. et al. // 1995. Quantum Electronics, vol.25, p.746.

Vagin N. P., et al. // 2003. Plazma Phys.Rep., vol.29. p.211.

Vagin N.P., et al. // 2004. Quantum Electron, vol.34, p.865.

Vagin N.P., et al. // 2006. Plazma Phys.Rep., vol.32, p.429.

Yuryshev N.N. // 1996. Quantum Electron., vol.26**,** p.567.

Yuryshev N.N. // 2001. "Electric discharge initiation of COIL with volume generation of atomic iodine", COIL R&D Workshop, 28-29 May 2001, Prague, Czech Republic.

Attachment 1:

List of published papers and reports with abstracts.

1. N.P.Vagin, A.A.Ionin, O.A.Rulev, L.V.Seleznev, D.V.Sinitsyn, N.N.Yuryshev. «The possibility study on realization of pulsed mode oxygen-iodine laser with electric discharge generator of singlet oxygen». High power lasers and high energy density physics. *Proc. of Int. Conf.* "X Khariton's scientific readings ", March 11-14, 2008, RFNC-VNIIEF, Sarov, Russia, 2008 (in Russian).

The opportunity of realization of electrically driven pulsed oxygen -iodine laser with a forced volume generation of iodine atoms has been studied. The negative role of oxygen atoms forming the effective quencher of singlet oxygen has been demonstrated by numerical simulation. The experiments performed showed the efficiency of relaxation processes is not too high as it was expected on the available kinetic information.

2. A.A.Ionin, Yu.M.Klimachev, A.A.Kotkov, A.Yu.Kozlov, I.V.Kochetov, A.P.Napartovich, O.A.Rulev, L.V.Seleznev, D.V.Sinitsyn, N.P.Vagin, N.N.Yuryshev. «Influence of Nitric Oxide Admixtures on Singlet Delta Oxygen Production in a Pulsed Electric Discharge for DOIL». International conference "Laser Optics 2008", June 23-28 St.Petersburg, Russia., Technical program.

The influence of nitrogen oxides on the specific input energy (SIE) and the time behavior of singlet delta oxygen (SDO) luminescence excited by a pulsed e-beam sustained discharge in oxygen were experimentally and theoretically studied. NO and NO_2 addition into oxygen results in a small increase and decrease in the SIE, respectively, the latter being connected with a large energy of electron affinity to NO_2. The addition of 0.1–0.3% nitrogen oxides was experimentally and theoretically demonstrated to result in a notable enhancement of the SDO lifetime, which is related to a decrease in the atomic oxygen concentration in afterglow.

3. N.N.Yuryshev, N.P.Vagin. «Experimental modeling the active medium of a pulsed DOIL with volume generation of iodine atoms». XVII International Symposium GCL/HPL2008, Lisbon, 15-19 September 2008 to be published in *SPIE Proceedings.*

The experimental modeling the active medium of pulsed DOIL has been performed by using the flow of iodide and chemically produced singlet oxygen with admixture of products formed in oxygen passing throw the discharge. The active medium was cooled by using dry ice to reduce the singlet oxygen threshold yield. Evaluation of an active medium temperature from photodissociation iodine laser parameters showed the cooling efficiency was high enough. The temperature down to 200K was obtained. It was observed the application of chemical singlet oxygen generator in the case of a deep cooling of active medium resulted in a decrease of initiation due to deposition of water vapour on the internal surface of a laser chamber. Taking into account this effect one can state the laser effect can be obtained at our experimental conditions at the singlet oxygen yield of about Y = 11%. The influence of discharge products on the laser performance was investigated. It was shown the methods used to remove the oxygen atoms from the flow from discharge were not effective. The ways for future investigations are discussed.

4. A.A.Ionin, Yu.M.Klimachev, A.A.Kotkov, A.Yu.Kozlov, I.V.Kochetov, A.P.Napartovich, O.A.Rulev, L.V.Seleznev, D.V.Sinitsyn, N.P.Vagin, N.N.Yuryshev. «Influence of Nitrogen Oxides on Singlet Delta Oxygen Production in Pulsed Electric Discharge for Oxygen-Iodine Laser». XVII International Symposium GCL/HPL 2008, Lisbon, 15-19 September 2008, to be published in *SPIE Proceedings.*

Nitrogen oxides NO and NO_2 influence of on the specific input energy and the time behavior of singlet delta oxygen (SDO) luminescence excited by a pulsed e-beam sustained discharge in oxygen were experimentally and theoretically studied. NO and NO_2 addition into oxygen results in a small increase and decrease in the specific input energy, respectively, the latter being connected with a large energy of

electron affinity to NO_2. The addition of 0.1–0.3% nitrogen oxides was experimentally and theoretically demonstrated to result in a notable enhancement of the SDO lifetime, which is related to a decrease in the atomic oxygen concentration in afterglow.

5. A.A.Ionin, Yu.M.Klimachev, A.Yu.Kozlov, A.A.Kotkov, I.V.Kochetov, A.P.Napartovich, O.A.Rulev, L.V.Seleznev, D.V.Sinitsyn, N.P.Vagin, N.N.Yuryshev. «Influence of nitrogen oxides on singlet delta oxygen production in pulsed discharge for electric discharge oxygen-iodine laser». *Bulletin of the American Physical Society*, **53**, (10), GW 3, 46-47 (2008).

Influence of nitrogen oxides NO and NO_2 on the specific input energy (SIE) and the time behavior of singlet delta oxygen (SDO) luminescence excited by a pulsed e-beam sustained discharge in oxygen were experimentally and theoretically studied. NO and NO_2 addition into oxygen results in a small increase and decrease in the SIE, respectively, the latter being connected with a large energy of electron affinity to NO_2. The addition of 0.1–0.3% nitrogen oxides was experimentally and theoretically demonstrated to result in a notable enhancement of the SDO lifetime, which is related to a decrease in the atomic oxygen concentration in afterglow.

6. A.A.Ionin, Yu.M.Klimachev, A.Yu.Kozlov, A.A.Kotkov, I.V.Kochetov, A.P.Napartovich, O.A.Rulev, L.V.Seleznev, D.V.Sinitsyn, N.P.Vagin, N.N.Yuryshev. «Influence of nitrogen oxides NO and NO_2 additives on singlet delta oxygen production in pulsed e-beam sustained discharge in oxygen». *Proc.SPIE*, **7005**, 70051J.

Experimental and theoretical study of influence of nitrogen oxides NO and NO_2 on the specific input energy (SIE) and the time behavior of singlet delta oxygen (SDO) luminescence excited by a pulsed e-beam sustained discharge in oxygen was carried out. NO and NO_2 addition into oxygen results in a small increase and decrease in the SIE, respectively, the latter being connected with a large energy of electron affinity to NO_2. The addition of 0.1–0.3% nitrogen oxides was experimentally and theoretically demonstrated to result in a notable enhancement of the SDO lifetime, which is related to a decrease in the atomic oxygen concentration in afterglow.

7. A.A.Ionin, Yu.M.Klimachev, O.A.Rulev, L.V.Seleznev, D.V.Sinitsyn. «Singlet delta oxygen production in RF discharge with transverse gas flow». Scientific MEPhI Session - 2009, Annotations of the reports, v. 2, p.230 (2009), Moscow, Russia (in Russian).

To study processes of production and relaxation of singlet delta oxygen (SDO) in gas flow excited by transverse periodically pulsed (frequency 100 Hz) slab RF discharge the experimental facility was created. The facility provided gas flow velocity up to 40 m/s at gas pressure up to 30 Torr with possibility of initial gas cooling before discharge area. Influence of RF discharge parameters, gas content, and pressure and gas flow of oxygen content gas mixture on gas temperature and temporal behavior of SDO luminescence was studied.

8. A.A.Ionin, Yu.M.Klimachev, A.Yu.Kozlov, A.A.Kotkov, I.V.Kochetov, A.P.Napartovich, O.A.Rulev, L.V.Seleznev, D.V.Sinitsyn, N.P.Vagin, N.N.Yuryshev. «Influence of nitrogen oxides NO and NO_2 on singlet delta oxygen production in pulsed discharge». *J. Physics D: Applied Physics*, **42**, 015201 (2009).

The influence of nitrogen oxides NO and NO_2 on the specific input energy (SIE) and the time behavior of singlet delta oxygen (SDO) luminescence excited by a pulsed e-beam sustained discharge in oxygen were experimentally and theoretically studied. NO and NO_2 addition into oxygen results in a small increase and decrease in the SIE, respectively, the latter being connected with a large energy of electron affinity to NO_2. The addition of 0.1–0.3% nitrogen oxides was experimentally and theoretically demonstrated to result in a notable enhancement of the SDO lifetime, which is related to a decrease in the atomic oxygen concentration in afterglow.

Attachment 2:

List of presentations at conferences and meetings with abstracts.

1. A.A.Ionin, Yu.M.Klimachev, A.Yu.Kozlov, A.A.Kotkov, I.V.Kochetov, A.P.Napartovich, O.A.Rulev, L.V.Seleznev, D.V.Sinitsyn, N.P.Vagin, N.N.Yuryshev. "Influence of nitrogen oxides on singlet delta oxygen production in pulsed discharge for electric discharge oxygen-iodine laser", 61-th Annual Gaseous Electronic Conference, October 13-17, 2008, Dallas, TX, USA.

Nitrogen oxides NO and NO_2 influence of on the specific input energy (SIE) and the time behavior of singlet delta oxygen (SDO) luminescence excited by a pulsed e-beam sustained discharge in oxygen were experimentally and theoretically studied. NO and NO_2 addition into oxygen results in a small increase and decrease in the SIE, respectively, the latter being connected with a large energy of electron affinity to NO_2. The addition of 0.1–0.3% nitrogen oxides was experimentally and theoretically demonstrated to result in a notable enhancement of the SDO lifetime, which is related to a decrease in the atomic oxygen concentration in afterglow.

2. A.A.Ionin, Yu.M.Klimachev, A.Yu.Kozlov, A.A.Kotkov, I.V.Kochetov, A.P.Napartovich, O.A.Rulev, L.V.Seleznev, D.V.Sinitsyn, N.P.Vagin, N.N.Yuryshev. "Influence of nitrogen oxides NO and NO_2 additives on singlet delta oxygen production in pulsed e-beam sustained discharge in oxygen", High Power Laser Ablation Conf., April 20-24, 2008, Taos, NM, USA (Invited)

Influence of nitrogen oxides NO and NO_2 on the specific input energy (SIE) and the time behavior of singlet delta oxygen (SDO) luminescence excited by a pulsed e-beam sustained discharge in oxygen were experimentally and theoretically studied. NO and NO_2 addition into oxygen results in a small increase and decrease in the SIE, respectively, the latter being connected with a large energy of electron affinity to NO_2. The addition of 0.1–0.3% nitrogen oxides was experimentally and theoretically demonstrated to result in a notable enhancement of the SDO lifetime, which is related to a decrease in the atomic oxygen concentration in afterglow.

3. A.A.Ionin, Yu.M.Klimachev, A.A.Kotkov, A.Yu.Kozlov, I.V.Kochetov, A.P.Napartovich, O.A.Rulev, L.V.Seleznev, D.V.Sinitsyn, N.P.Vagin, N.N.Yuryshev. "Influence of nitric oxide admixture on singlet delta oxygen production in pulsed electric discharge for DOIL", Int. Conf. "Laser Optics 2008", June 23-28, 2008, S.Petersburg, Russia.

Experimental and theoretical study of influence of nitrogen oxides NO and NO_2 on the specific input energy (SIE) and the time behavior of singlet delta oxygen (SDO) luminescence excited by a pulsed e-beam sustained discharge in oxygen was carried out. NO and NO_2 addition into oxygen results in a small increase and decrease in the SIE, respectively, the latter being connected with a large energy of electron affinity to NO_2. The addition of 0.1–0.3% nitrogen oxides was experimentally and theoretically demonstrated to result in a notable enhancement of the SDO lifetime, which is related to a decrease in the atomic oxygen concentration in afterglow.

4. A.A.Ionin, Yu.M.Klimachev, O.A.Rulev, L.V.Seleznev, D.V.Sinitsyn. «Singlet delta oxygen production in RF discharge with transverse gas flow». Scientific MEPhI Session - 2009, January 26-30, 2009, Moscow, Russia (in Russian).

To study processes of production and relaxation of singlet delta oxygen (SDO) in gas flow excited by transverse periodically pulsed (frequency 100 Hz) slab RF discharge the experimental facility was created. The facility provided gas flow velocity up to 40 m/s at gas pressure up to 30 Torr with possibility of initial gas cooling before discharge area. Influence of RF discharge parameters, gas content, and pressure and gas flow of oxygen content gas mixture on gas temperature and temporal behavior of SDO luminescence was studied.

5. A.A.Ionin, Yu.M.Klimachev, A.Yu.Kozlov, A.A.Kotkov, I.V.Kochetov, A.P.Napartovich, O.A.Rulev, L.V.Seleznev, D.V.Sinitsyn, N.P.Vagin, N.N.Yuryshev. “Influence of Nitrogen Oxides on Singlet Delta Oxygen Production in Pulsed Electric Discharge for Oxygen-Iodine Laser”, VII International Symposium on Gas Flow and Chemical Lasers & High Power Lasers, 15-19 September 2008, Lisbon, Portugal.

The influence of nitrogen oxides NO and NO_2 on the specific input energy (SIE) and the time behavior of singlet delta oxygen (SDO) luminescence excited by a pulsed e-beam sustained discharge in oxygen were experimentally and theoretically studied. NO and NO_2 addition into oxygen results in a small increase and decrease in the SIE, respectively, the latter being connected with a large energy of electron affinity to NO_2. The addition of 0.1–0.3% nitrogen oxides was experimentally and theoretically demonstrated to result in a notable enhancement of the SDO lifetime, which is related to a decrease in the atomic oxygen concentration in afterglow.

6. N.P.Vagin, A.A.Ionin, O.A.Rulev, L.V.Seleznev, D.V.Sinitsyn, N.N.Yuryshev. «The possibility study on realization of pulsed mode oxygen-iodine laser with electric discharge generator of singlet oxygen». High power lasers and high energy density physics. International Conference "X Khariton's scientific readings ", March 11-14, 2008, Sarov, Russia (in Russian).

The features of singlet oxygen kinetics in an active medium of an electrically driven oxygen-iodine laser have been examined. The parameters of experimental facility have been investigated. The possibility of obtaining the lasing threshold at 11% of singlet oxygen yield has been demonstrated with a chemical singlet oxygen generator.

7. N.N.Yuryshev, N.P.Vagin. “Experimental modeling the active medium of a pulsed DOIL with volume generation of iodine atoms”, VII International Symposium on Gas Flow and Chemical Lasers & High Power Lasers, 15-19 September 2008, Lisbon, Portugal.

It was demonstrated with a chemical singlet oxygen generator the effluents of MW discharge in oxygen did not quench singlet oxygen totally at the stage of laser chamber filling. The similar conclusion can be made on the base of results of investigation of influence of MW discharge parameters on the pulse of a photolytically initiated iodine laser on the mixture of iodide with effluents of MW discharge in oxygen.

Attachment 3:

Information on patents and copy rights.

There were no claims for a patent.

RUSSIAN ACADEMY OF SCIENCES
Физический институт имени П.Н.Лебедева
Ф И А Н

ISTC Project No. 3835-P

Study of factors determining the gain characteristics of DOIL active medium

Final Project Technical Report

on the work performed from March 01, 2008 to February 28, 2009

P.N.Lebedev Physical Institute of Russian Academy of Sciences,
N.G.Basov Quantum Radiophysics Institute

Project Manager **Ionin Andrey Alekseevich,**
Professor

Director	**Krokhin Oleg Nikolaevich, Academician**	